DIFFUSION OF ENTRAPPED GAS FROM POROUS MEDIA

by

Kenneth M. Adam and Arthur T. Corey

April 1968

HYDROLOGY PAPERS
COLORADO STATE UNIVERSITY
Fort Collins, Colorado

27

Several departments at Colorado State University have substantial research and graduate programs oriented to hydrology. These Hydrology Papers are intended to communicate in a fast way the current results of this research to the specialists interested in these activities. The papers will supply most of the background research data and results. Shorter versions will usually be published in the appropriate scientific and professional journals.

This research was conducted by the Agricultural Engineering Department, Colorado State University. Funds were provided through National Science Foundation Research Grant No. GK-689.

DIFFUSION OF ENTRAPPED GAS FROM POROUS MEDIA

by

Kenneth M. Adam and Arthur T. Corey

HYDROLOGY PAPERS

COLORADO STATE UNIVERSITY

FORT COLLINS, COLORADO

April 1968 No. 27

ABSTRACT

The purpose of this study was to develop and test equations that describe the process whereby a gas which is in isolated pockets surrounded by a liquid, diffuses from a porous media and is replaced by liquid. The equation developed by Bloomsburg for the case of unidirectional diffusion and a similar equation developed by introducing one simplifying assumption beyond those made by Bloomsburg were tested. Experimental results show that neither of these developments adequately describe the process.

A graphical method developed from observing the trends of experimental data is given. It is based upon extrapolation of experimental data obtained using cores obtained from the material of interest. Besides giving the time at which full liquid saturation would occur, this method allows the liquid distribution to be estimated at any time from normalized curves which relate air content to dimensionless length, using dimensionless time as a parameter.

ACKNOWLEDGMENTS

This paper is primarily based on research performed by K.M. Adam under the direction of A.T. Corey during study towards a Doctor of Philosophy degree at Colorado State University. The research was supported by the U.S. National Science Foundation, whose support is gratefully acknowledged.

The present study was preceded by the work of G. L. Bloomsburg which is described in Colorado State University Hydrology Paper No. 5. The present authors are grateful for the work and ideas presented by Bloomsburg.

The authors wish to express their appreciation to Dr. W.D. Kemper, Department of Agronomy, Colorado State University for reviewing an initial draft of this paper.

TABLE OF CONTENTS

LIST OF TABLES

LIST OF FIGURES

NOTATION AND DEFINITIONS

Symbol	Definition	Dimensions
A	Area	L^2
a	A constant	none
b	Slope or a constant	none
C	Excess concentration of dissolved gas (above that which is in equilibrium with the atmosphere)	ppm by mass
C_o	Assumed uniform excess concentration of dissolved gas (above that which is in equilibrium with the atmosphere) in a liquid in a porous medium. It is computed from the bubbling pressure	ppm by mass
C_B	Excess concentration of dissolved gas (above that which is in equilibrium with the atmosphere) at the exterior boundary of the core	ppm by mass
C_t	Excess concentration of dissolved gas (above that which is in equilibrium with the atmosphere) in the volume element dV at any given time	ppm by mass
D	Coefficient of diffusion of dissolved gas in a liquid	L^2/T
D_e	Effective coefficient of diffusion; $D_e = \frac{D}{T^2}$	L^2/T
F	Flow rate of gas by diffusion	L^3/L^2T
F_1	Flow rate of gas by diffusion through the fully saturated zone of the core	L^3/L^2T
F_2	Flow rate of gas by diffusion through the front separating the saturated and unsaturated zone	L^3/L^2T
g	Acceleration due to gravity	L/T^2
h	Bubbling pressure head in centimeters of liquid	L
h_m	Bubbling pressure head in millimeters of mercury	L
i	Denotes a "dummy variable"	none
j	Denotes a "dummy variable"	none
j-k	Denotes a "dummy variable"	none
K	Saturated permeability - permeability of a porous medium to a liquid which completely fills all pore spaces - sometimes called intrinsic permeability	L^2
k	Denotes a confidence level	none
K_r	Relative permeability - the permeability at any saturation divided by the fully saturated permeability	none
L	Length	L
L_e	Effective length - distance traversed by a differential fluid element in moving between two points in a porous medium	L
M	Mass	FT^2/L
M_t	Mass flow rate	FT/L
n	Denotes a "dummy variable"	none

Symbol	Definition	Dimensions
N	Denotes the number of counts on decade scaler	None
P	Pressure	F/L^2
P_b	Bubbling pressure - the smallest capillary pressure on the drainage cycle at which gas permeability is greater than zero	F/L^2
P_c	Capillary pressure - pressure in the gas minus the pressure in the liquid	F/L^2
P_g	Pressure of gas	F/L^2
P_ℓ	Pressure of liquid	F/L^2
q	Denotes a "source"	ppm/Time
r	Radius of curvature	L
S	Wetting fluid saturation, equal to the volume of liquid divided by the volume of voids	none
S_o	Initial saturation - the saturation when gas becomes entrapped	none
T	Absolute temperature	^oK
T^2	Tortuosity; $(L_e/L)^2$	none
t	Time	T
t_o	Time when diffusion process begins	T
t_s	Time when sample becomes fully saturated	T
$t.$	A dimensionless time	none
v	Liquid volume flux	L^3/L^2T
V	Volume	L^3
V_a	Volume of air in a porous medium at any time	L^3
V_{ao}	Initial volume of entrapped air in a porous medium	L^3
V_f	Volume of air which has diffused from the porous medium at any time $(V_{ao} - V_a)$	L^3
V_ℓ	Volume of liquid in a porous medium	L^3
W	Weight of sample and liquid phase at any saturation	F
W_o	Weight of sample and liquid when initial conditions exist	F
W_s	Weight of sample and liquid at full saturation	F
x	A length variable	L
x_s	Denotes the length of the saturated region	L
α	Proportionality constant	L/T
α_i	Constant of linear equation	none
β_i	Slope of linear equation	none
Δ	Denotes a difference	none
ζ	A "dummy variable"	none

Symbol	Definition	Dimensions
η	A pore size distribution index	none
μ^2	"Square microns", a unit of permeability	L^2
ρ	Fluid mass density	FT^2/L^4
ρ_a	Mass density of gas at atmospheric pressure	FT^2/L^4
ρ_{ab}	Mass density of air in entrapped pockets	FT^2/L^4
ρ_ℓ	Mass density of liquid	FT^2/L^4
σ	Interfacial tension of liquid in contact with gas	F/L
$\sigma_{d.s.}$	Interfacial tension of distilled water	F/L
σ_s	Interfacial tension of Soltrol	F/L
τ	A "dummy variable"	none
ϕ	Porosity - the volume of pore space expressed as a fraction of bulk volume of the medium	none

DIFFUSION OF ENTRAPPED GAS FROM POROUS MEDIA[1]

Kenneth M. Adam and Arthur T. Corey[2]

INTRODUCTION

Entrapped gas affects the behavior of fluid systems in porous media. Examples are encountered in many geological and biological structures. It is widely known that a flowing liquid will remove gas from a porous medium either by dissolution of the gas into the flowing liquid or by the bulk transport of gas bubbles. The fact that gas in isolated pockets which is surrounded by an essentially static liquid, diffuses from a porous medium under the influence of interfacial energy is often not recognized. The phenomenon is not understood sufficiently to permit an analytical solution of the rate of diffusion of gas from the medium.

In 1964, Bloomsburg and Corey (4) published the results of a study which indicated that a cylindrical sample of a porous medium, enclosed to allow diffusion from one end only, but free to take in liquid from the other end, will gain weight with time and will eventually become fully saturated. By measuring the properties of a variety of samples and observing the weight of these samples as a function of time as liquid replaced the gas, an insight into the variables affecting this process was gained.

From this insight and a theoretical analysis, Bloomsburg hypothesized that the part of the sample which first becomes fully saturated with liquid is at the surface from which the gas escapes. Furthermore, it was theorized that the zone of complete saturation would advance toward the interior as a fairly abrupt front. Based upon these assumptions and others, Bloomsburg derived an equation describing the rate at which the process proceeds. This equation did not describe the observed experimental behavior quantitatively. Furthermore, the equation contained a parameter that had to be obtained from the observation of the process itself. Nevertheless, dimensionless parameters obtained from Bloomsburg's theoretical equation indicated that the equation did have some merit.

Bloomsburg's experimental procedure did not provide a test of the basic assumptions as to how the process of diffusion proceeded.

The study reported here was designed to test Bloomsburg's hypothesis of an abrupt front of complete saturation and to derive, if possible, more satisfactory equations describing the rate of escape of entrapped gas.

Characteristics of media affecting the rate of diffusion include the external geometry of the sample and the internal geometry of the sample as determined by pore size and pore-size distribution. Other factors include the fluid properties such as density of the liquid and the gas, the solubility and diffusivity of the gas in the liquid, and the surface tension of the liquid. The factors that apparently determine the amount of entrapped gas are the pore-size distribution, the shape, smoothness and cleanliness of the particles that constitute the medium. Another factor which affects both the amount of entrapped gas and rate of escape of the gas is the fluctuation of ambient pressure.

---

[1]Contribution from the Agricultural Engineering Department, Colorado State University.

[2]Assistant Professor, University of Manitoba, Winnipeg, Manitoba, formerly a graduate student at Colorado State University; Professor of Agricultural Engineering, Colorado State University, Fort Collins, Colorado, respectively.

BACKGROUND

Corey (8) became interested in the study of entrapped gas as a result of efforts to estimate the quantity of natural gas recoverable from porous geological formations by water flooding. While working for Gulf Research and Development Corporation, he attempted to develop ways of making such an estimation by causing small rock samples to imbibe liquid and measuring the amount of liquid imbibed. By weighing the samples periodically to determine the quantity of liquid contained in the pores, he determined that gas temporarily entrapped in the rocks (through which there was no liquid flowing but which was in contact with a liquid supply) slowly disappeared from the porous media.

It was observed that covering the lateral surface of a cylindrical rock core decreased the rate at which gas disappeared. It was also observed that although the gas gradually was replaced entirely by liquid, the gas could not have moved out by bulk flow since (at this stage of saturation) the rocks had zero conductivity to gas. Corey concluded that the disappearance of the gas was a diffusion process.

Bloomsburg and Corey (4) observed that during an experiment to obtain permeability as a function of P_c on the imbibition cycle, permeability continued to increase slowly for 11 days at a constant value of capillary pressure after the permeability had appeared to reach a maximum. This phenomenon is shown in Figure 1. In this figure, permeability is expressed as relative permeability, K_r, that is, the permeability at any saturation as a ratio of the permeability at full saturation. Evidently, a slow increase in saturation occurred as a result of diffusion of entrapped air into the flowing liquid. This occurred even though the liquid was previously saturated with air at the external air pressure.

Bloomsburg and Corey attempted to describe the diffusion process analytically. Their theory was based upon the following concepts and assumptions:

1. The interfacial forces acting at a liquid-gas interface result in a pressure difference across the interface given by

$$\Delta P = \sigma\left(\frac{1}{r_1} + \frac{1}{r_2}\right) \qquad (1)$$

where ΔP is the pressure difference, σ is the interfacial tension, and r_1 and r_2 are any mutually perpendicular radii of curvature of the interface. Adam (1), Davies and Rideal (9), and Rouse (24) have presented derivations of this equation. The pressure difference ΔP is often called capillary pressure P_c,

$$P_c = P_g - P_\ell \,, \qquad (2)$$

P_g being the pressure of the gas and P_ℓ the pressure of the liquid.

2. The internal geometry of a porous medium is adequately characterized by the bubbling pressure,

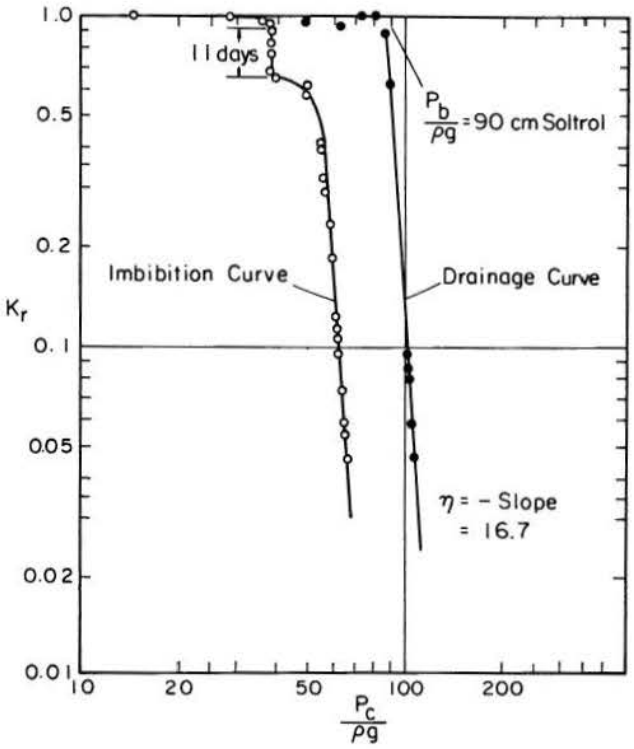

Figure 1. Relative permeability as a function of capillary pressure head for determination of $P_b/\rho g$ and η

pore-size distribution index, and permeability. The bubbling pressure, P_b, is defined as the minimum capillary pressure on the drainage cycle at which the gas permeability is greater than zero. The pore-size distribution index, η, is the negative slope of the curve of permeability as a function of capillary pressure on logarithmic paper. Figure 1 shows that each of these parameters may be obtained from such a curve, as Brooks and Corey (5) have proposed.

3. Henry's law applies. This law states that the equilibrium concentration of dissolved gas in a liquid is proportional to the partial pressure of the gas in contact with the liquid. It was assumed that the liquid is in contact with the atmosphere for a long period of time and that the liquid has an initial concentration of dissolved air which is in equilibrium with the atmosphere.

4. All of the entrapped gas pockets have interfaces with equivalent curvatures. Pockets of gas at higher than atmospheric pressure tend to dissolve into the liquid. Since the pockets with smaller radii contain higher pressure, they dissolve fastest, producing a higher concentration of the gas in solution than is in equilibrium with gas pockets with larger radii. The gas, therefore, tends to collect in the largest pockets which are characterized by the bubbling pressure.

5. The flux of gas from the exterior surface is proportional to the excess concentration of gas in the liquid at the exterior surface. Excess concentration is the concentration above that which is in equilibrium with the partial pressure of the gas beyond the exterior surface. This concentration is obviously a time dependent variable.

6. The zone of complete saturation advances through the medium as a fairly abrupt front.

7. The flux of gas through the zone of complete saturation is proportional to the gradient of concentration of dissolved gas.

8. The concentration of dissolved gas in the zone of complete saturation varies linearly, consequently, the concentration gradient is constant at any particular time within the zone of complete saturation.

9. The porous media consisted of homogeneous and isogropic material. A liquid was assumed to have imbibed into the media trapping gas uniformly throughout. All surfaces of the media were assumed to be wetted by the liquid, and all gas pockets were assumed to be completely surrounded by the liquid.

These concepts and assumptions allowed Bloomsburg to derive the expression

$$\frac{V_f}{V_{ao}} = \left[\left(\frac{D}{\alpha L}\right)^2 + \frac{2C_o}{(1-S_o)\phi}\,\frac{\rho_\ell}{\rho_a}\,\frac{Dt}{L^2}\right]^{\frac{1}{2}} - \frac{D}{\alpha L} \qquad (3)$$

for the case of unidirectional diffusion of entrapped gas, where V_f is the volume of gas that has diffused from the core at any time, t, V_{ao} is the volume of gas originally trapped in the sample, D is the diffusion coefficient of the gas in the liquid. α is the constant of proportionality relating flux rate to concentration at the exterior face, L is the length of the sample, C_o is the excess concentration in the unsaturated region, S_o is the initially imbibed saturation, ϕ is the porosity of the medium and ρ_ℓ and ρ_a are the mass density of the liquid and gas respectively at atmospheric pressure.

Bloomsburg recognized that the coefficient of diffusion, D, contained in Equation (3), should be corrected for the tortuosity of the liquid paths and the porosity of the porous medium. However, there is no generally accepted method of calculating a correction factor. A correction factor based on tortuosity at high saturations and porosity is constant for a particular media. Bloomsburg elected, therefore, to analyze the data by using the coefficient of diffusion of the gas in the liquid rather than a corrected value.

In order to test Equation (3), Bloomsburg studied consolidated cores of porous materials including sandstones, ceramics and glass beads. The length, diameter, dry weight, porosity, bubbling pressure and pore-size distribution index were tabulated for each sample. Soltrol[1] "C" core test fluid was used as the liquid in some sandstone cores, and water was used in the sandstone, ceramic and glass bead cores.

The cores were sealed around the lateral surface with impervious adhesive tape and placed in a vertical position with the lower end free to imbibe the liquid. They were kept inside a closed plastic container so that there was little evaporation from the exposed surface of the core. There was always liquid in the bottom of the container so that the air in the container was saturated with liquid vapor.

Shortly after the wetting front reached the top of the cores, the cores were removed, the inlet ends were "blotted" to remove excess liquid and they were weighed. It was observed that a fairly rapid increase in saturation occurred for a short time. Bloomsburg attributed this increase to air dissolving from the small pockets. The weights of the samples were recorded as a function of time.

The experimental data collected by Bloomsburg allowed saturation to be plotted as a function of time. These data indicated that Soltrol trapped less air in a given core than did water. Among the cores of similar materials, there appeared to be less gas trapped in the cores with higher bubbling pressure and higher η values; however, there were exceptions to this. Shape and smoothness might have been the most important variable affecting the amount of trapped gas since glass beads had the least gas trapped. When water was the imbibing fluid, wetability may have been equally important.

Equation (3) was given as the theoretical equation for the unidirectional diffusion case. Bloomsburg observed from the equation that as the time variable became large relative to $(D/\alpha L)^2$ that a curve of V_f/V_{ao} as a function of $(Dt/L^2)^{\frac{1}{2}}$ would approach a straight line of slope

$$\left(\frac{2C_o\rho_\ell}{(1-S_o)\phi\rho_a}\right)^{\frac{1}{2}} .$$

According to the theory, this straight line should intersect the time axis at $V_f/V_{ao} = -D/\alpha L$. Bloomsburg reasoned, also, that because of two factors the slope might deviate from that indicated by the theory. These two factors are: (1) the concentration C_o itself is computed from the bubbling pressure of the medium, and (2) the value of D used is affected by the tortuosity of the liquid paths and the porosity of the porous medium.

A small number of data of V_f/V_{ao} as a function of $(Dt/L^2)^{\frac{1}{2}}$ was presented for each curve. In most cases the data did approach a straight line which intersected the axis for zero time at negative values of V_f/V_{ao}. There were exceptions to this; in fact, for three out of eleven cores presented, this intercept was positive. From the same plots Bloomsburg observed that larger values of

$$\frac{2C_o\rho_\ell}{(1-S_o)\rho_a} ,$$

which is the theoretical parameter times the porosity, did correspond to steeper slopes. Only one exception occurred within the sandstone cores; that sample had a low value of η which would indicate a wide range of pore sizes. In this case the assumption of uniform interface curvatures was probably not valid.

[1] Soltrol "C" core test fluid, Phillips Petroleum Company, Special Products Division, Barlesville, Oklahoma.

Other than the work of Bloomsburg and Corey (4) and Corey (8), there has been no literature found concerning the diffusion process. Many articles have been written on related subjects. The authors are aware of several articles (6, 15, 20, 22, 26) specifically concerned with the effect of entrapped air on permeability. Others (2, 3, 10, 11, 13, 14, 17, 18, 19) have been concerned with dissolution of bubbles into a liquid or growth of a bubble with various boundary conditions. Soil scientists and hydrologists (21,23) have studied the effect of confined air on infiltration.

CRITIQUE AND THEORETICAL CONSIDERATIONS

The theoretical equation derived by Bloomsburg (Equation 3) can be rearranged to show that

$$x = \left[\left(\frac{D}{\alpha}\right)^2 + \frac{2C_o}{(1-S_o)\phi}\frac{\rho_\ell}{\rho_a} Dt\right]^{\frac{1}{2}} - \frac{D}{\alpha} \quad , \tag{4}$$

x being a distance from the exterior face to the end of the fully saturated region. This indicates that the saturated zone proceeds inward from the exterior face and that the rate of advance is independent of the length of the sample. This is to be expected considering the development of Equation (3).

It is apparent that a simple experiment would have provided a test of the validity of Equation (4). That is, two samples of the same material, but of different lengths would be expected to gain weight on a unit cross-sectional area basis at the same rate. Bloomsburg did not use two samples of the same material with different lengths. Furthermore, the data from each sample was presented as saturation as a function of time. If the process had proceeded as Bloomsburg predicted, the saturation at any time would have been dependent on the sample length. Thus, a better variable might have been weight gain per unit area $(W - W_o)/A$, where W_o is the weight of liquid in the sample when initial conditions exist. This variable is sufficient to characterize the process regardless of whether or not Equation 3 was valid.

An interesting characteristic of the variable $(W - W_o)/A$ is that when it is divided by $(W_s - W_o)/A$, where W_s is weight of liquid in the sample, the ratio V_f/V_{ao} is obtained. That is,

$$\frac{V_f}{V_{ao}} = \frac{W - W_o}{W_s - W_o} \tag{5}$$

Furthermore,

$$\frac{V_f}{V_{ao}} = \frac{S - S_o}{1 - S_o} \quad , \tag{6}$$

since

$$\frac{V_f}{V_{ao}} = \frac{W - W_o}{W_s - W_o} = \frac{\frac{W}{W_s} - \frac{W_o}{W_s}}{\frac{W_s}{W_s} - \frac{W_o}{W_s}} = \frac{S - S_o}{1 - S_o} \quad .$$

The ratio V_f/V_{ao} is independent of how the volumes of air are compared, provided that the volumes are compared either both at atmospheric pressure or both at the pressure corresponding to that inside the pockets. Bloomsburg evidently assumed that the pressure increase in the pockets would affect the density of the air by only a negligible amount. Considering that this pressure increase is the mechanism initiating the diffusion, such an assumption may not be appropriate. Furthermore, considering the material of highest bubbling pressure employed by Bloomsburg, i.e., 90 cm of oil, the maximum air density would be

$$\rho_{ab} = 1.08\ \rho_a \tag{7}$$

where ρ_{ab} is the density of air in the pockets.

In the development of Equation (3), Bloomsburg used the ratio ρ_ℓ/ρ_a to convert the concentration of dissolved air in parts per million by mass to concentrations by volume. Since the density of air, ρ_a, was the density at atmospheric pressure, the flow rates are on the basis of volumes at atmospheric pressure. The continuity equation given by Bloomsburg is

$$V_a = V_{ao} - \frac{\rho_\ell}{\rho_a}\int_o^{V_\ell} C_t dV - A\alpha\frac{\rho_\ell}{\rho_a}\int_o^t C_B d\tau \quad , \tag{8}$$

where V_a is the volume of gas in the sample at time t, C_t is the excess dissolved gas concentration in the elemental volume dV, A is the cross-sectional area of flow, and C_B is the excess dissolved gas concentration at the exterior face as a function of time. It should be noted that the last two terms are on the basis of volumes of air at atmospheric pressures whereas V_a and V_{ao} are at pressures corresponding to the bubbling pressure of the particular sample. Using Bloomsburg's assumption that the bubbling pressure is the excess pressure inside the pockets, the continuity equation becomes

$$\frac{\rho_{ab}}{\rho_a} V_a = \frac{\rho_{ab}}{\rho_a} V_{ao} - \int_o^{V_\ell} C_t dV - A\alpha\frac{\rho_\ell}{\rho_a}\int_o^t C_B d\tau, \tag{9}$$

or

$$\frac{\rho_{ab}}{\rho_a} V_f = A\alpha\frac{\rho_\ell}{\rho_a}\int_o^t C_B d\tau, \tag{10}$$

again neglecting the term

$$\frac{\rho_\ell}{\rho_a}\int_o^{V_\ell} C_t dV$$

since it is small. Equation (3), therefore, becomes

$$\frac{V_f}{V_{ao}} = \left[\left(\frac{D}{\alpha L}\frac{\rho_{ab}}{\rho_a}\right)^2 + \frac{2C_o}{(1-S_o)\phi}\frac{\rho_\ell}{\rho_a}\frac{Dt}{L^2}\right]^{\frac{1}{2}} - \frac{D}{\alpha L}\frac{\rho_{ab}}{\rho_a} \quad . \tag{11}$$

The term

$$\frac{\rho_\ell}{\rho_a}\int_o^{V_\ell} C_t dV \quad ,$$

was disregarded by Bloomsburg on the grounds that it was small in comparison to the volume of liquid, V_ℓ.

The comparison, however, should be to the volume of air originally trapped. Since the smallest initial saturation obtained by Bloomsburg was 0.75,

$$V_{ao} = (1-S_o)\ V_\ell = 0.25\ V_\ell \quad , \qquad (12)$$

which indicates that the term perhaps should not have been neglected.

When the last pocket of entrapped gas dissolves into the liquid, the sample is fully saturated. Immediately after complete saturation, however, an excess concentration of gas exists throughout the sample and a considerable period of time is required before all the liquid in the sample has a concentration of gas that is in equilibrium with the partial pressure of gas exterior to the sample. This excess concentration comprises over half of the volume originally dissolved. Since this volume of air is neglected after the disappearance of the last pockets of gas, it seems reasonable to neglect it at the beginning of the process. Considering that the sample contains more liquid at the end than at the beginning of the process, Bloomsburg's assumption might be acceptable. Moreover, if the volume of gas originally trapped is defined as that volume of air that occupies the sample after the excess concentration has been dissolved, the omission of a term accounting for this volume is appropriate, remembering that a comparable amount of dissolved gas remains in the sample after the gas pockets have disappeared.

It was unfortunate that of the sixteen samples used by Bloomsburg, only three attained full saturation. Nevertheless, it is possible to compare his experimental results with the theoretical equation for unidirectional diffusion. Analysis of Equation (3) as derived by Bloomsburg, that is,

$$\frac{V_f}{V_{ao}} = \left[\left(\frac{D}{\alpha L}\right)^2 + \frac{2C_o}{(1-S_o)}\,\frac{\rho_\ell}{\rho_a}\,\frac{Dt}{L}\right]^{\frac{1}{2}} - \frac{D}{\alpha L}$$

indicates that when $t = t_s$, $V_f/V_{ao} = 1$, where t_s is the time at complete saturation. Consequently, it is possible to solve for the constant of proportionality α , which relates the surface concentration C_B to the volume flux, giving

$$\alpha = \frac{2D}{L}\left[\frac{1}{\dfrac{2C_o}{(1-S_o)\phi}\,\dfrac{\rho_\ell}{\rho_a}\,\dfrac{Dt_s}{L^2} - 1}\right] . \qquad (13)$$

Since α is the only unknown in this equation, its numerical value can be obtained and substituted into Equation (3). This would permit a comparision of the theoretical and experimental ratios of V_f/V_{ao} at intermediate times.

The authors have reason to believe, however, that the experimental results obtained by Bloomsburg are incompatible with his mathematical model. Figure (2) shows that for the same material, Bloomsburg's experimental method allowed liquid intake (or gas outflow) at a faster rate than when the diffusion is truly unidirectional. Bloomsburg placed the samples in a vertical position in a thin layer of liquid with the lateral surfaces sealed by adhesive. This was not sufficient to induce unidirectional diffusion, however. Although the process was one-dimensional, the diffusion occurred in two directions, despite being somewhat restricted at the end on which the sample was supported. For this reason, Bloomsburg did not attain experimentally the conditions assumed for the mathematical model.

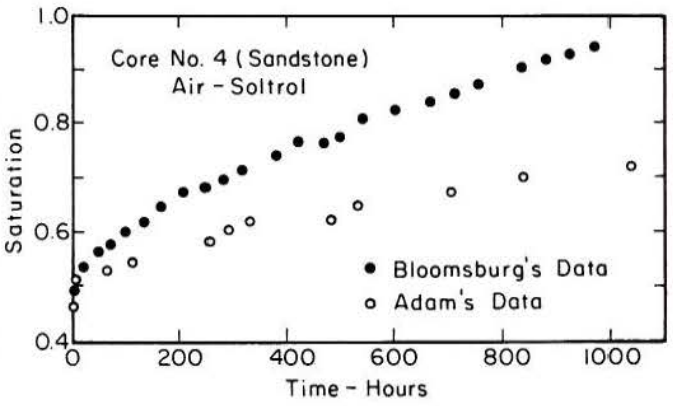

Figure 2. Typical curve of saturation as a function of time

It is interesting to consider a mathematical model similar to that of Bloomsburg, except that the excess concentration on the exterior face, C_B , is assumed to be zero. This assumption may be a close approximation, except at small times, since there may be no significant accumulation of excess gas in solution at the exterior face with this experimental arrangement. In the actual case, the concentration must decrease from the uniform initial excess concentration, C_o , at the exterior face to some low excess concentration which approaches zero after some period of time.

Support is given to such an assumption by the work of Hawke and Parts (16). They found that the resistance offered by the surface layer of water molecules to the passage of hydrogen sulfide molecules was zero within their experimental error. This presumably indicates that the exterior layer of molecules of a liquid provides little resistance to diffusion in comparison to the resistance through the entire liquid phase.

Proceeding with the assumption that C_B is zero, and referring to the model as shown below,

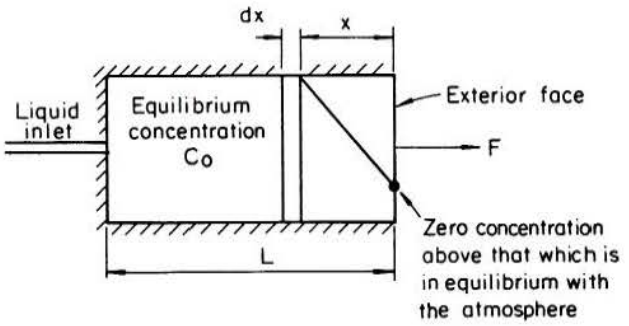

Figure 3. Model for unidirectional diffusion

the following relationship can be written:

$$F_1 = -\frac{D_e C_o}{x}\frac{\rho_\ell}{\rho_a} \qquad (14)$$

where F_1 is the volume flux of gas per unit area at the exterior face, and D_e is a corrected coefficient of diffusion known as the effective coefficient of diffusion. Also,

$$F_2 = -\frac{V_{ao}}{V}\frac{dx}{dt} \qquad (15)$$

or

$$F_2 = -(1-S_o)\phi\frac{dx}{dt} \quad ,$$

since

$$\frac{V_{ao}}{V} = (1-S_o)\phi \quad ,$$

where F_2 is the volume flux of gas per unit area through the area separating the fully saturated and partially saturated zones. Assuming that the gas coming out of solution in the region x is negligible, F_1 and F_2 may be equated. Thus,

$$\frac{D_e C_o}{x}\frac{\rho_\ell}{\rho_a} = (1-S_o)\phi\frac{dx}{dt}$$

or

$$\frac{D_e C_o \rho_\ell}{(1-S_o)\rho_a}\int_o^t d\tau = \int_o^x \zeta d\zeta \; .$$

Integrating, it is found that

$$x = \left[\frac{2C_o D_e}{(1-S_o)\phi}\frac{\rho_\ell}{\rho_a}\right]^{\frac{1}{2}}(t)^{\frac{1}{2}} \; . \qquad (17)$$

Dividing both sides of the equation by L, and remembering that $x/L = V_f/V_{ao}$, the result is

$$\frac{V_f}{V_{ao}} = \left[\frac{2C_o}{(1-S_o)}\frac{\rho_\ell}{\rho_a}\right]^{\frac{1}{2}}\left[\frac{D_e t}{L^2}\right]^{\frac{1}{2}} \; . \qquad (18)$$

This analysis yields the same result as Bloomsburg's equation for large times. That is, a plot of V_f/V_{ao} as a function of $[D_e t/L^2]^{\frac{1}{2}}$ should yield straight lines of slope $2C_o\rho_\ell/(1-S_o)\phi\rho_a$. Since the process of diffusion of entrapped gas is very slow and the period of interest is when liquid saturation is nearly complete, it is possible that Equation (18) would usually suffice. The validity of Equations (3) and (18) is discussed later.

It should be noted that both Equations (3) and (18) were derived on the assumption that a linear concentration distribution exists in the saturated zone. Theoretically, such a condition cannot exist with a moving boundary such as that under consideration. A linear distribution cannot exist in such a case because as the concentration changes with time, some mass of dissolved gas must come out of solution. Consequently, the flux must increase as the exterior face is approached from the interior of the sample and the concentration gradient would be expected to increase near the exterior.

The problem can be described in a strict mathematical sense by a boundary value problem, that is,

$$C_t(x,t) = D_e C_{xx}(x,t) + q(x,t)$$

$$C(0,t) = 0 \qquad C(x,0) = C_o \qquad (19)$$

$$C_x(L,t) = 0$$

where the subscript notation means that the variable is partially differentiated with respect to that subscript, C is the concentration and $q(x,t)$ is an unknown source term. For a Fourier solution by the separation of variables method as discussed by Churchill (7), $q(x,t)$ must be known. This term, of course, would have to be such as to describe the emission of the gas mass from the entrapped pockets. Such a solution would give the distribution of concentration within the sample. That is, $C(x,t)$ would be known in terms of a Fourier series solution. Regardless of the nature of such a solution, an assumption to relate the mass rate of escape of gas from the exterior face to the volume of entrapped pockets would still be required. The mass flow rate could be obtained from the expression

$$M_t = -AD \text{ grad } C(x,t)\big|_{x=0} \qquad (20)$$

where M_t is the mass flow at $x = 0$ for any time, t, and A is the area of the exterior face. As previously mentioned, the above method of solution would require, as a prerequisite, an adequate mathematical description of the source term. Such a term would have the dimensions of mass of gas per unit mass of liquid per unit of time. Mathematically, it would be such that

$$q(x,t) = 0 \qquad (x < x_s)$$

$$q(x,t) = q(x,t) \qquad (x > x_s)$$

$$q(L,t_s) = 0$$

where x_s is the region of complete saturation.

It is conceivable that if such a function were known that the function itself would permit a solution to the overall problem. This would result from the fact that the source strength in a region where there is no entrapped gas would be zero. Furthermore, it is probable that the source strength in any region where there is entrapped gas depends on the curvature of the interfaces. The curvature of interfaces probably could be related to the liquid saturation to provide the desired solution. A rigorous analytical description of the diffusion process, however, does not appear to be possible without additional knowledge of the source term.

EXPERIMENTAL TECHNIQUES

The experimental methods used were designed to test the validity of Bloomsburg's equation, while gaining an insight into the process of diffusion of entrapped gas. The preparation of all samples to test Bloomsburg's equation required that boundary conditions be imposed on each sample such that unidirectional diffusion would prevail.

The liquid used in all experiments was either Soltrol "C" or distilled water. The gas used in each experiment was either air or nitrogen. Soltrol "C" was used in the majority of experiments since it has more consistent wetting qualities than water, and its surface tension is not as readily changed by contaminants. Thus, it was expected that initial saturation would be more consistent with the use of this fluid, along with a more consistent diffusion process. Distilled water, with 12.5 parts per million mercuric chloride added, was used to verify that analogous results could be expected with different liquids. Mercuric chloride was added to the distilled water to prevent growth of algae which tend to obstruct pores. Also, algae tend to add weight to a sample, thus interfering with saturation measurements.

Nitrogen was used in some cases instead of air as the gaseous phase upon the recommendation of G. L. Bloomsburg. He proposed that a pure gas be used instead of air to simplify the determination of the solubility and diffusivity of the gas in the liquid, air being a mixture of gases. No significant difference was detected, however, either in solubility or diffusivity between air in Soltrol and nitrogen in Soltrol. Furthermore, based on the use of three samples, no statistical difference was found in the experimental data when nitrogen was used instead of air in two out of three cases tested. Considering that air is composed of 78% nitrogen, such results are not surprising. For convenience, air was used in the majority of experiments.

The porous media used in the experiments were alundum, diatomaceous earth and a variety of sandstones. All samples were consolidated cores of lengths from four to twenty centimeters and diameters of approximately 2.5 centimeters. Alundum is a ceramic material supplied by Coors Porcelain Company, Golden, Colorado. Diatomaceous earth is an artificially constructed consolidated material made of special clays. This material was supplied by the Allen Filter Company, Industrial Products Division, Toledo, Ohio.

All the required properties of water, Soltrol, air and nitrogen were known except for the solubility and diffusivity of nitrogen in Soltrol. Bloomsburg had previously obtained these values for air in Soltrol.

The method of obtaining these constants was the same as that used by Bloomsburg and described in Appendix A of the paper by Bloomsburg and Corey (4). An improvement was made in the experimental apparatus by placing the liquid container in a temperature bath so as to control the temperature of the liquid within $\pm$ 0.05°C. The purpose of this temperature control was to eliminate errors in the diffusivity value caused by convective circulation of the liquid. This circulation does not affect solubility. Figure 4 shows the solubility data obtained by Bloomsburg and the author which indicate no significant difference in the solubilities of air and nitrogen in Soltrol. Figure 5 shows the experimental data of Bloomsburg for the diffusivity of air in Soltrol and the data of the author for nitrogen in Soltrol. These data are calculated on the basis of $D = 15 \times 10^{-5}$ cm^2/sec . On the basis of Bloomsburg's assumption that at any given time the experimental ratio of M/M_∞ cannot be less than the theoretical value, the value of D is close to 15×10^{-5} cm^2/sec . The value of 16×10^{-5} cm^2/sec, therefore, was chosen as the diffusivity coefficient, D , for nitrogen in Soltrol. The value used for diffusivity of air in water was 2×10^{-5} cm^2/sec . The data obtained to determine the diffusivity of nitrogen in Soltrol were based on four similar but independent trials. The data of a particular trial, however, do not constitute statistically independent data points, and thus do not meet the requirements of most statistical tests. Many more trials would be required for other types of statistical tests.

The length, diameter, area, bulk volume, dry weight, saturated weight and porosity were measured or calculated for each sample. The saturated permeability, K , bubbling pressure head, $P_b/\rho g$, and pore-size distribution index, n , were then found experimentally. These parameters were obtained from capillary pressure-permeability experiments. Table 1 gives an example of

TABLE 1. CAPILLARY PRESSURE - PERMEABILITY DATA FOR ALUNDUM 360

Temp °C	$\mu/\rho g \times 10^5$ cm/sec	$\frac{\Delta H}{\Delta L}$	$v \times 10^4$ cm/sec	K μ^2	K_r	$P_c/\rho g$ mm of Soltrol
25.0	1.945	0.915	3.30	0.704	1.00	21.2
25.5	1.927	0.945	3.51	0.715	1.01	51.2
25.0	1.945	1.020	3.70	0.708	1.00	66.2
24.8	1.952	1.060	3.86	0.680	0.973	87.2
25.0	1.945	1.153	3.62	0.591	0.835	91.3
24.8	1.942	1.162	2.05	0.333	0.470	95.1
24.6	1.959	1.634	1.20	0.139	0.196	99.2
25.0	1.945	2.090	0.738	0.0666	0.0940	103.3
25.0	1.945	1.658	0.0338	0.00383	0.0054	120.0

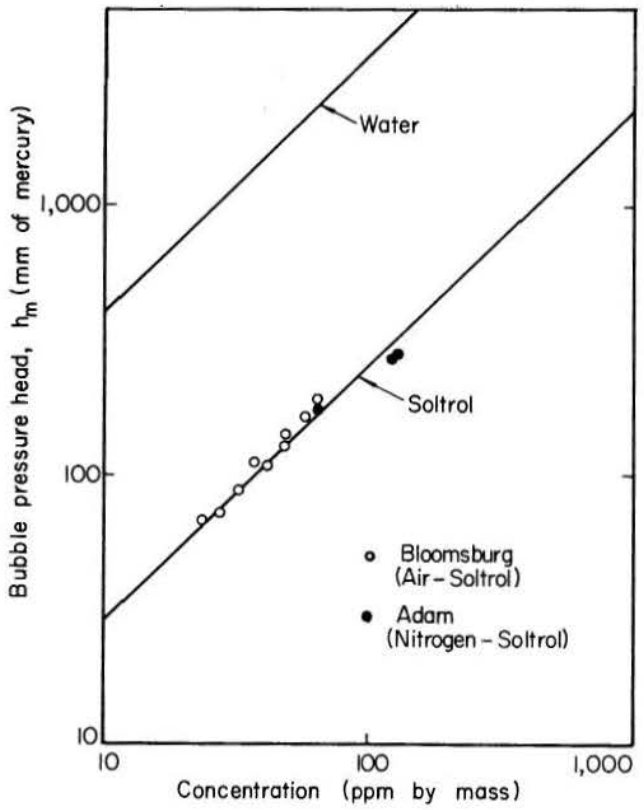

Figure 4. Solubility data

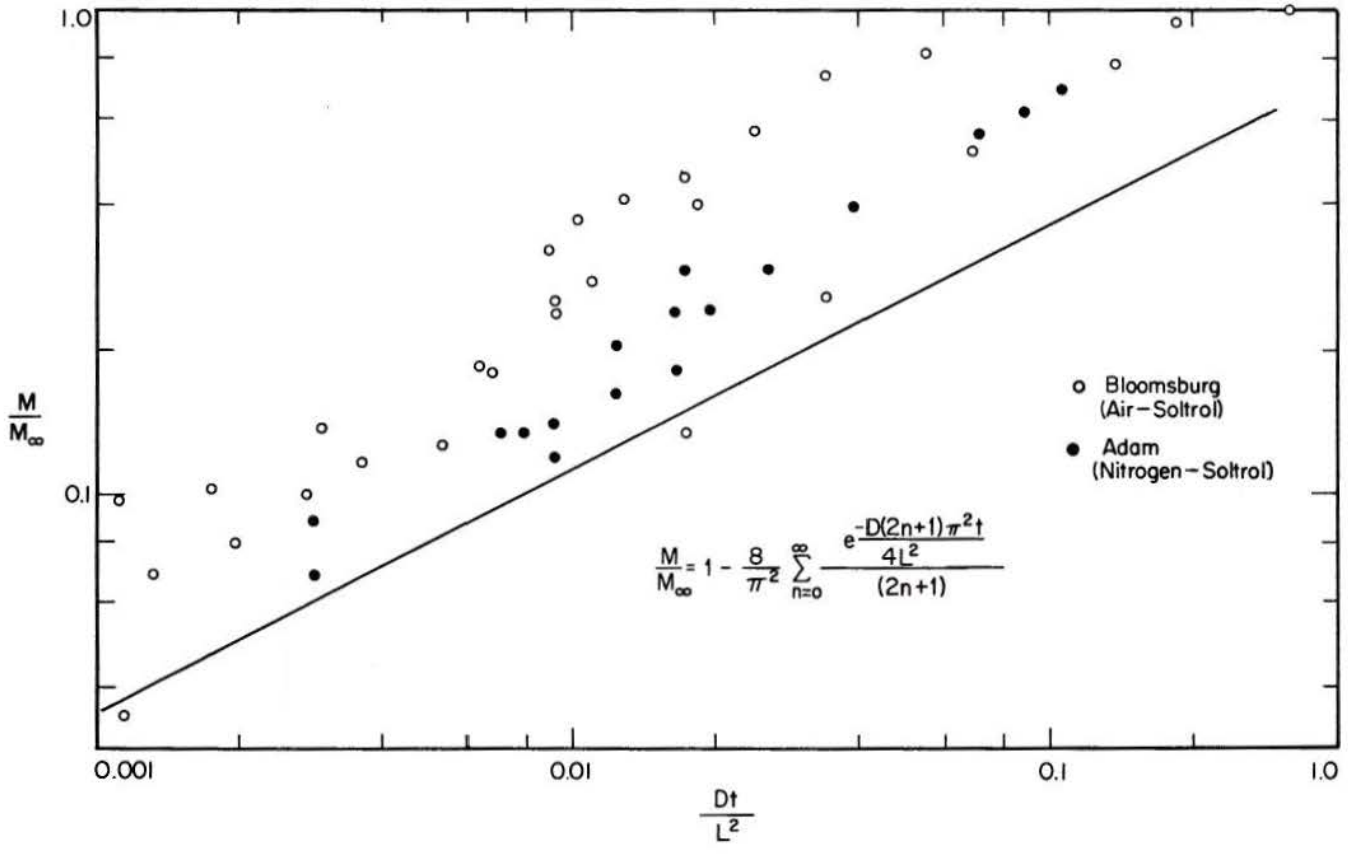

Figure 5. Diffusivity data

the data from such an experiment. Figure 6 shows the data and the resultant parameters.

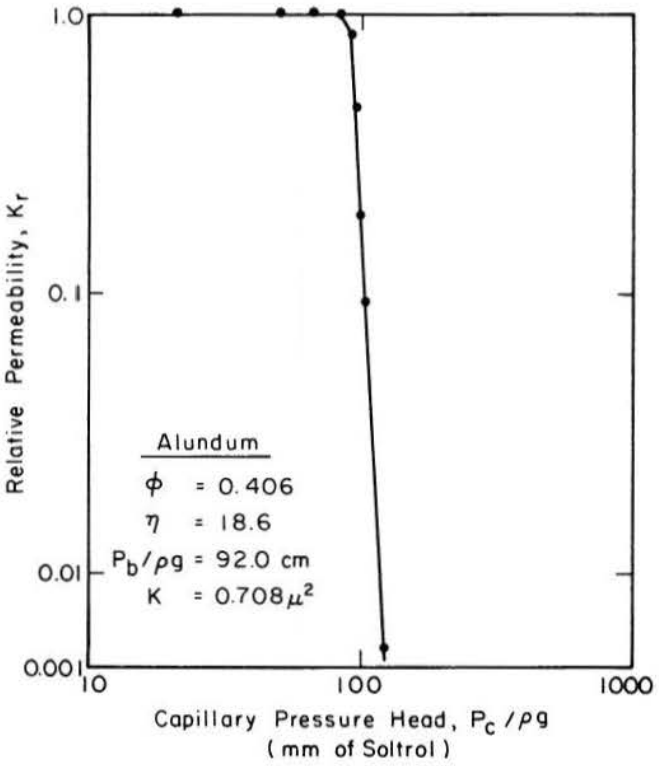

Figure 6. Relative permeability as a function of capillary pressure for Alundum 360

The samples were then wrapped with thin aluminum sheeting held in place by an epoxy resin. One end was not sealed. In the other end an opening comprising approximately 1% of the total end area was drilled through the aluminum and adhesive. This allowed the entrance of the liquid, while preventing a significant amount of diffusion from that end. This procedure insured that unidirectional diffusion existed in each sample. A sketch of a prepared sample is shown in Figure 7.

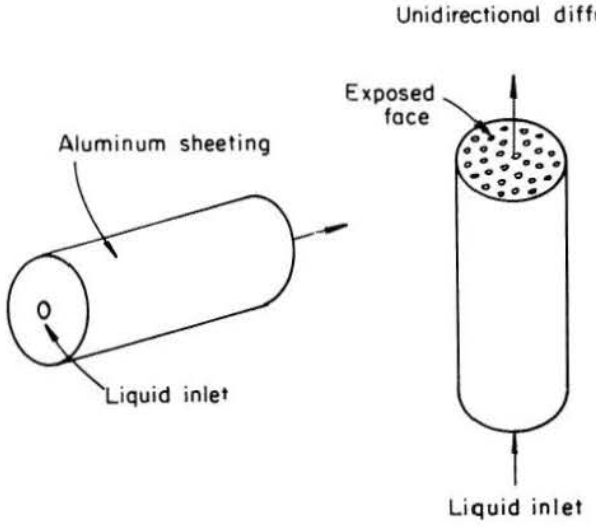

Figure 7. Sketchs of a prepared sample

Samples 8 to 14 inclusive were prepared additionally by placing transparent lucite end caps over each end and sealing the circumferential joints. A sketch of such a prepared sample is shown in Figure 8.

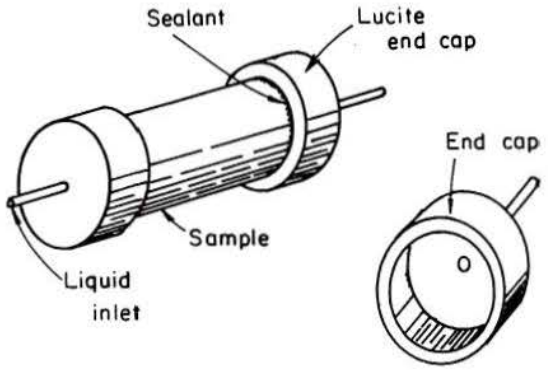

Figure 8. Sketchs of the end caps on a prepared sample

After each sample was fully prepared its dry, fully saturated, and imbibed saturation weights were recorded.

Two types of experiments were performed with these samples. The simplest experiment consisted of placing the prepared samples, without end caps, in a thin layer of liquid contained in a transparent box. The samples were placed in a vertical position resting on the end in which the small inlet hole existed. The upper end was fully exposed so that diffusion could occur from that end. The box was covered so that essentially no evaporation occurred from the exposed end. Such samples were weighed periodically and the time was recorded.

The more complex experiment utilized the samples complete with end caps. The inlet cap, which was filled with liquid, contained a small screw at the top which covered an outlet for the liquid chamber. This outlet was necessary in order to remove any gas that formed in this chamber. The gas usually appeared in the liquid chamber when the samples were weighed. Some of this gas, however, was the result of back diffusion through the small liquid inlet. The other end cap contained a small screw at the bottom which served as a drainage outlet for the gas chamber. This drainage outlet was necessary since a drop or two of liquid would enter the gas chamber as a result of the slight elevation head that existed when the samples were in the horizontal position. It was necessary to remove this liquid prior to weighing the sample each time.

The inlet and outlet caps were connected so that equal pressure existed throughout the system. This was required as a result of fluctuations in barometric pressure. When the outlet end was connected to a closed gas collection chamber and the inlet end was left open to the atmosphere, large fluctuations in sample weight occurred. The two ends were connected by a calibrated glass tube filled with liquid on the inlet end and a flexible tube completing the closed system. A negligible pressure difference existed across the gas-liquid interface in the inlet tube.

The purpose of the sample being arranged in a horizontal position was to facilitate the determination of the liquid distribution by use of low energy gamma

radiation. The sample, which was arranged in a closed system, as shown in Figure 9, was placed between an Americium 241 low energy gamma source and a scintillation detector. The scintillation detector contained a sodium iodide crystal which is particularly sensitive to low energy radiation. Upon striking this crystal, the radiation energy is converted to light photons. Each flash of light is detected by a photomultiplier tube and converted to an electrical pulse. This impulse is amplified and transmitted to an external instrument.

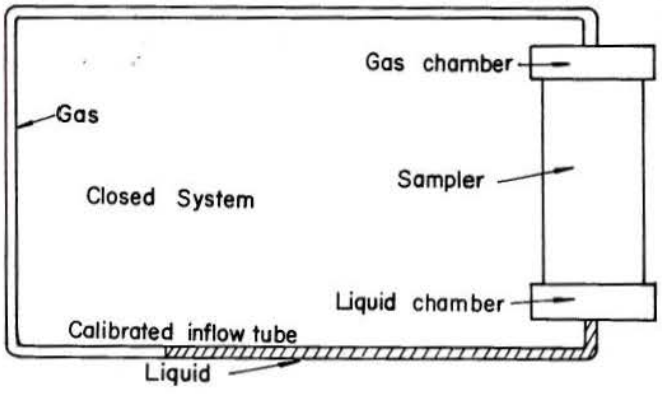

Figure 9. Diagram of the closed system sample prepared for gas distribution determination

The counting instrument used in this experiment was a Nuclear-Chicago Decade Scaler, Model 186. Such a scaler is designed to count and indicate the number of pulses received from an external pulse-type nuclear radiation detector. The assembly of equipment is shown in Figure 10.

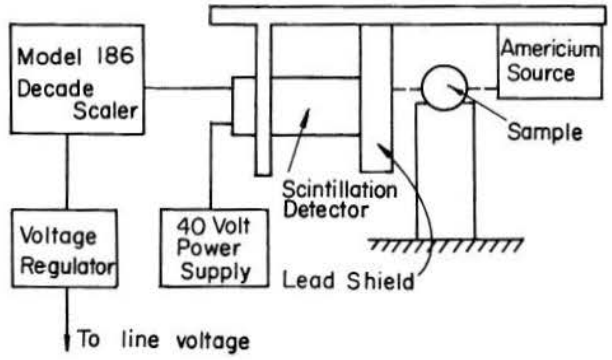

Figure 10. Apparatus assembly for the gas distribution determination

This equipment made it possible to locate and measure the quantity of entrapped gas along the axis of the sample. The principle of the equipment is that the adsorption of gamma radiation is proportional to the mass through which it passes. The greater the amount of entrapped gas at any position along the axis of the sample, the greater the amount of radiation that passes through the sample from a constant source. The relation between mass and count rate allowed a calibration to be made at each position along a sample. The count rate, when the sample was at known saturations, was determined for each position. From these data a graph of count rate as a function of saturation was obtained for each position. The calibration of the six samples studied in this manner required approximately 500 such graphs. A typical graph of count rate as a function of saturation is shown in Figure 11.

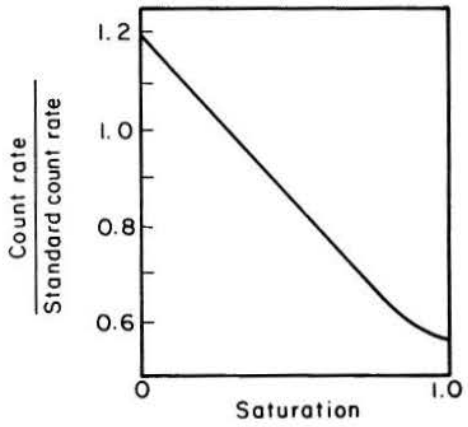

Figure 11. Typical calibration curve of count rate as a function of saturation

The shape of the curve in Figure 11 has been found by other investigators. Ferguson (12) and others have found that count rate as a function of moisture content, or saturation, is a linear relationship at low saturations. At high saturations, smaller differences in count rate occur for equal increments of saturation as the saturation approaches unity. It is unfortunate that this occurs, since in this case it is the range of high saturation which is of interest. This results in less accuracy. It is estimated that individual saturation values could be in error by as much as ± 4.0%. The estimate of error for an individual saturation value at a point along the axis of the sample was based on probability theory. According to this theory, the error associated with the average value determined from a sample of random counts is inversely proportional to the square root of the total number of counts, or

$$\text{error} = \frac{k}{\sqrt{N}}$$

where k reflects the confidence in the computed error and N is the total number of counts. Using the 99% confidence level, it was estimated that 1% of the time an error exceeding ± 4% saturation was obtained.

All experiments were performed in a room with temperature control of ± 2°C.

RESULTS AND DISCUSSION

The physical dimensions and properties of all cores are tabulated in Table 2. These data were obtained at 25° ± 2°C. The last three columns in Table 2, the hypothetical pore radius, r, the initial concentration, C_o, and the time at full saturation, t_s, previously have not been explained.

TABLE 2. MATERIAL PROPERTIES

Core No.	Material	Wetting Fluid	Nonwetting Fluid	Length (cm)	Diameter (cm)	Area (cm^2)	Dry Weight (grams)	Prepared Dry Weight (grams)	Fully Saturated Weight (grams)	S_o (dimensionless)
1	Sandstone	Soltrol	Air	4.86	2.54	5.065	54.20	56.80	56.80	0.637
2	Sandstone	Soltrol	Air	4.52	2.53	5.025	49.90	51.25	54.40	0.810
3	Sandstone	Soltrol	Air	4.47	2.52	4.985	46.62	47.92	51.76	0.674
4	Sandstone	Soltrol	Air	5.49	2.54	5.065	61.49	64.43	67.64	0.474
5	Sandstone	Soltrol	Air	4.56	2.48	4.828	42.07	44.56	48.95	0.736
6	Sandstone	Soltrol	Air	4.51	2.54	5.065	52.45	53.59	55.88	0.472
7	Sandstone	Soltrol	Air	4.78	2.54	5.065	53.16	56.15	59.02	0.477
8	Alundum-98	Soltrol	Air	6.03	2.72	5.850	77.98	80.30	90.43	0.637
9	Alundum-360	Soltrol	Air	5.90	2.72	5.850	74.15	90.69*	100.97	0.694
10	Alundum-360	Soltrol	Air	20.40	2.72	5.850	254.60	291.68*	327.95**	0.741
11	Diatomaceous Earth	Soltrol	Nitrogen	6.27	2.53	5.025	20.98	48.70*	65.64	0.897
12	Diatomaceous Earth	Soltrol	Nitrogen	6.27	2.53	5.025	20.98	50.20*	67.14	0.901
13	Diatomaceous Earth	Soltrol	Air	6.27	2.53	5.025	20.98	48.65*	65.59	0.899
14	Diatomaceous Earth	Soltrol	Air	20.40	2.56	5.140	80.60	116.42*	171.12	0.871
15	Diatomaceous Earth	Soltrol	Air	6.30	2.57	5.187	21.98	25.13	42.50	0.927
16	Diatomaceous Earth	Soltrol	Air	6.30	2.57	5.187	21.98	25.13	42.49	0.927
17	Diatomaceous Earth	Soltrol	Air	6.30	2.57	5.187	21.98	25.13	42.48	0.927
18	Diatomaceous Earth	Soltrol	Air	6.30	2.57	5.187	21.98	25.13	42.50	0.927
19	Diatomaceous Earth	Water	Air	4.84	2.48	4.812	18.06	20.16	34.36	0.952
20	Diatomaceous Earth	Water	Air	4.89	2.37	4.405	16.28	18.48	31.82	0.936
21	Diatomaceous Earth	Water	Air	4.90	2.53	5.013	18.72	21.00	36.00	0.951
22	Diatomaceous Earth	Water	Air	4.72	2.40	4.529	16.66	19.15	32.50	0.933

Core No.	Sample Weight at S_o, W_o (grams)	Porosity ϕ (dimensionless)	$\frac{P_b}{\rho g}$ (cm of liquid)	$\frac{P_b}{\rho g}$ Converted to mm of Mercury	η (dimensionless)	K (cm^2 x 10^8)	Hypothetical Pore Radius (cm^2)	C_o (ppm)	t_s (hrs)
1	61.29	0.379	49	27.2	17.9	1.99	0.00128	11.5	4213.0
2	53.80	0.183	80	44.4	5.7	0.0136	0.000775	18.5	683.0
3	50.51	0.228	78	43.3	11.4	0.0377	0.000800	18.0	1059.0
4	65.95	0.153	44	24.4	3.9	0.0023	0.0014	10.2	3725.0
5	47.79	0.264	53	29.4	8.4	0.167	0.00118	12.3	941.0
6	54.67	0.133	48	26.6	13.5	0.155	0.00130	11.0	2165.0
7	57.52	0.157	46	25.5	7.5	0.172	0.00135	10.8	2561.0
8	86.75	0.378	46	25.5	15.1	1.90	0.00135	10.8	4701.0
9	97.82	0.406	92	51.1	18.6	0.708	0.000682	21.4	5667.0
10	318.54	0.406	92	51.1	18.6	0.708	0.000682	21.4	6681.0*
11	63.89	0.707	800	444.1	3.0	0.0927	0.0000780	185.0	395.1
12	65.47	0.707	800	444.1	3.0	0.0927	0.0000780	185.0	360.0**
13	63.88	0.707	800	444.1	3.0	0.0927	0.0000780	185.0	504.3
14	164.05	0.688	800	444.1	3.0	0.0927	0.0000780	185.0	3022.0
15	41.23	0.703	800	444.1	3.0	0.0927	0.0000780	185.0	250.1***
16	41.22	0.703	800	444.1	3.0	0.0927	0.0000780	185.0	425.6
17	41.21	0.703	800	444.1	3.0	0.0927	0.0000780	185.0	426.9
18	41.23	0.703	800	444.1	3.0	0.0927	0.0000780	185.0	415.0
19	33.68	0.610	1600	444.1	3.0	0.0927	0.000240	11.22	505.0
20	30.97	0.620	1600	444.1	3.0	0.0927	0.000240	11.22	529.0
21	35.27	0.611	1600	444.1	3.0	0.0927	0.000240	11.22	529.0
22	31.60	0.625	1600	444.1	3.0	0.0927	0.000240	11.22	529.0

*End caps on sample and inlet end full of liquid
**Calculated value
***Prepared by Bloomsburg's method

The hypothetical radius is a computed value, its magnitude being inversely proportional to the bubbling pressure. The equation for the pressure difference across a spherical bubble is assumed to apply. That is,

$$\Delta P = \frac{2\sigma}{r} \tag{21}$$

or

$$r = \frac{2\sigma}{\Delta P} = \frac{2\sigma}{\rho g h} \tag{22}$$

where ρ is the density of the liquid, and h is the bubbling pressure head in centimeters of liquid. For convenience, if h is expressed in millimeters of mercury, the result is

$$r = \frac{2\sigma}{1.36\ g h_m} \tag{23}$$

where h_m is the bubbling pressure head in millimeters of mercury, σ is the surface tension for the two fluids involved, and r is the hypothetical radius in centimeters. Using the surface tension and density for Soltrol as σ_s = 23 dynes/cm and ρ_s = 0.755 gm/cm, and for distilled water as $\sigma_{d.s.}$ = 72 dynes/cm and $\rho_{d.s.}$ = 0.997 gms/cm , respectively, the hypothetical pore radius is given as a function of bubbling pressure head in millimeters of mercury in Figure 12.

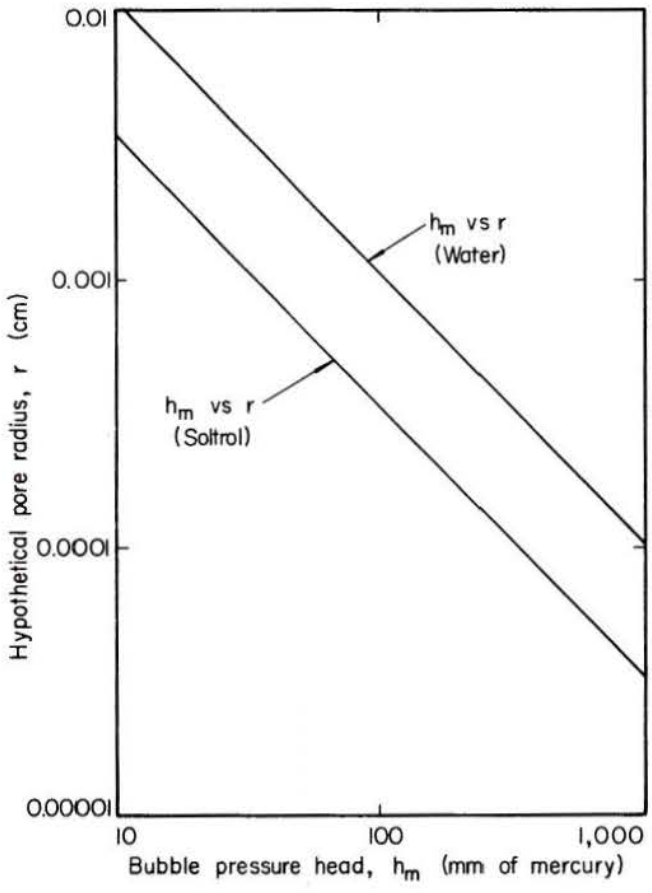

Figure 12. Hypothetical pore radius as a function of bubbling pressure head

The value of C_o can be obtained directly from the solubility data as given in Figure 4. This graph gives the value of C_o as a function of the bubbling pressure head in millimeters of mercury. The values of solubility of air in water were supplied by Dr. W. D. Kemper of the Agronomy Department at Colorado State University. The final column in Table 4 gives the time required by each sample to reach full saturation.

The assumption that the concentration in the partially saturated region reaches some equilibrium value C_o has been justified by Bloomsburg. Support for this assumption is found in the fact that for most materials a graph of capillary pressure as a function of saturation indicates that capillary pressure changes only slightly over a considerable range of the higher saturations. A curve of capillary pressure head as a function of saturation is given in Figure 13 which shows the typical shape of such curves on the drainage cycle. Although curves on the imbibition cycle are directly applicable to the case under consideration, such curves cannot be obtained experimentally for saturations greater than the saturation at which gas is entrapped.

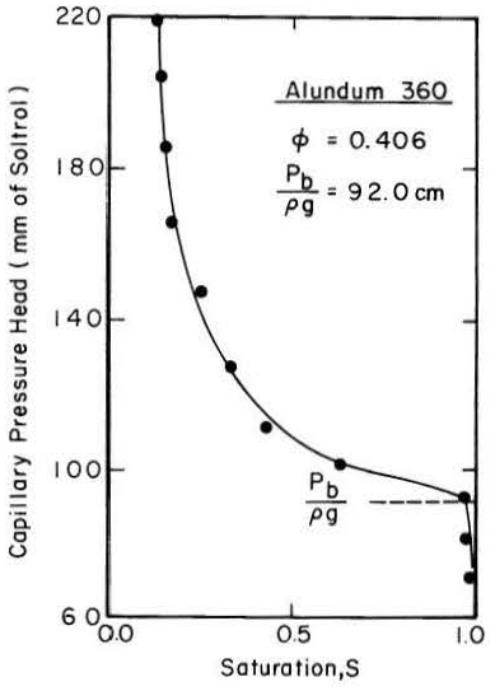

Figure 13. Typical curve of capillary pressure as a function of saturation

This indicates that in the range of saturation of interest in the present study the capillary pressure changes only over a small range, and, moreover, it does not deviate appreciably from the bubbling pressure. Since the concentration is directly related to the pressure, the assumption that the concentration remains constant in the unsaturated region, seems reasonable. Based on experimental data which are presented later, however, it appears that a concentration gradient must exist in the partially saturated region, and therefore the concentration cannot be constant throughout this region, although the gradient may be slight.

The curves of weight as a function of time are presented in Figure 14. The data from which these

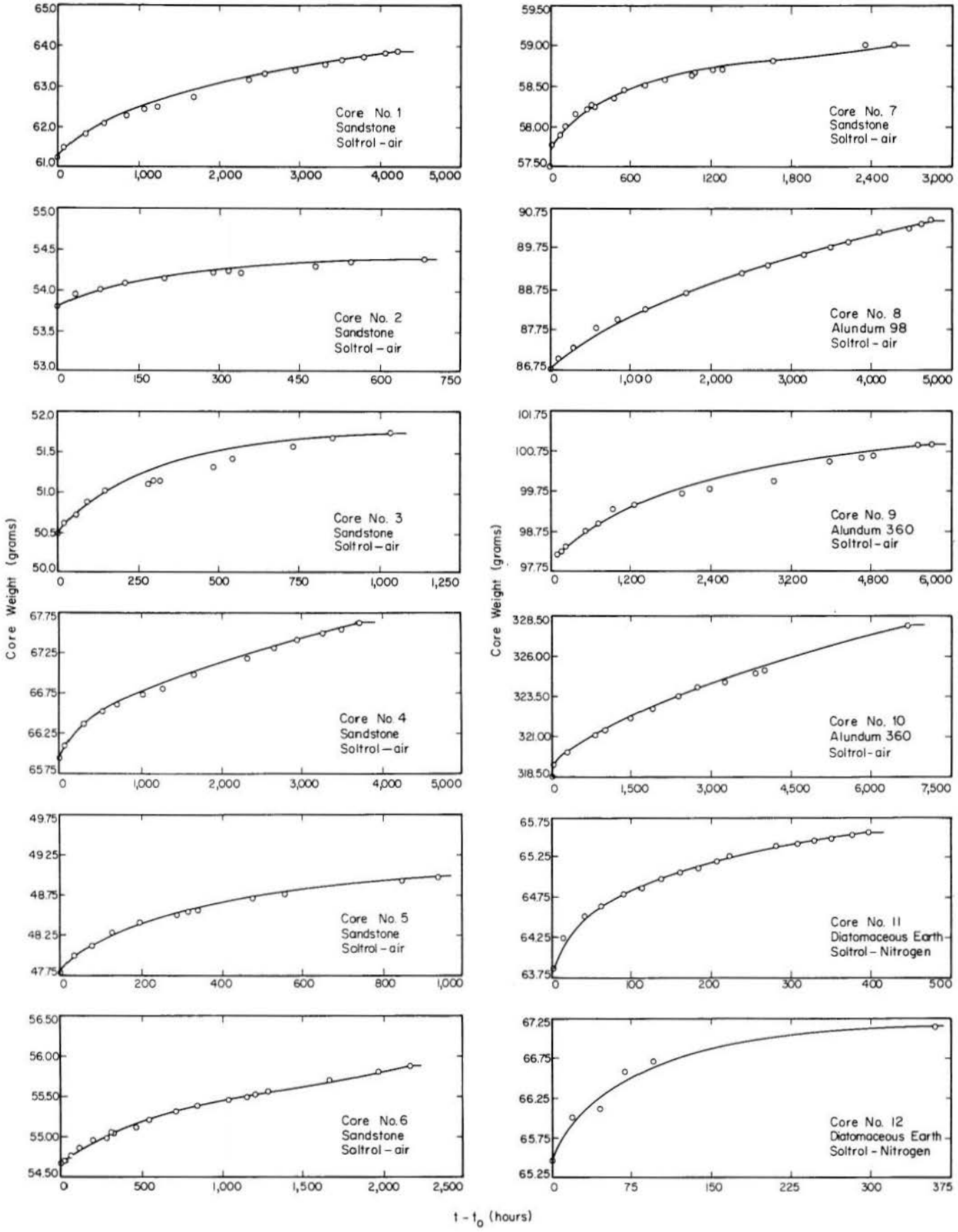

Figure 14. Core weight as a function of time

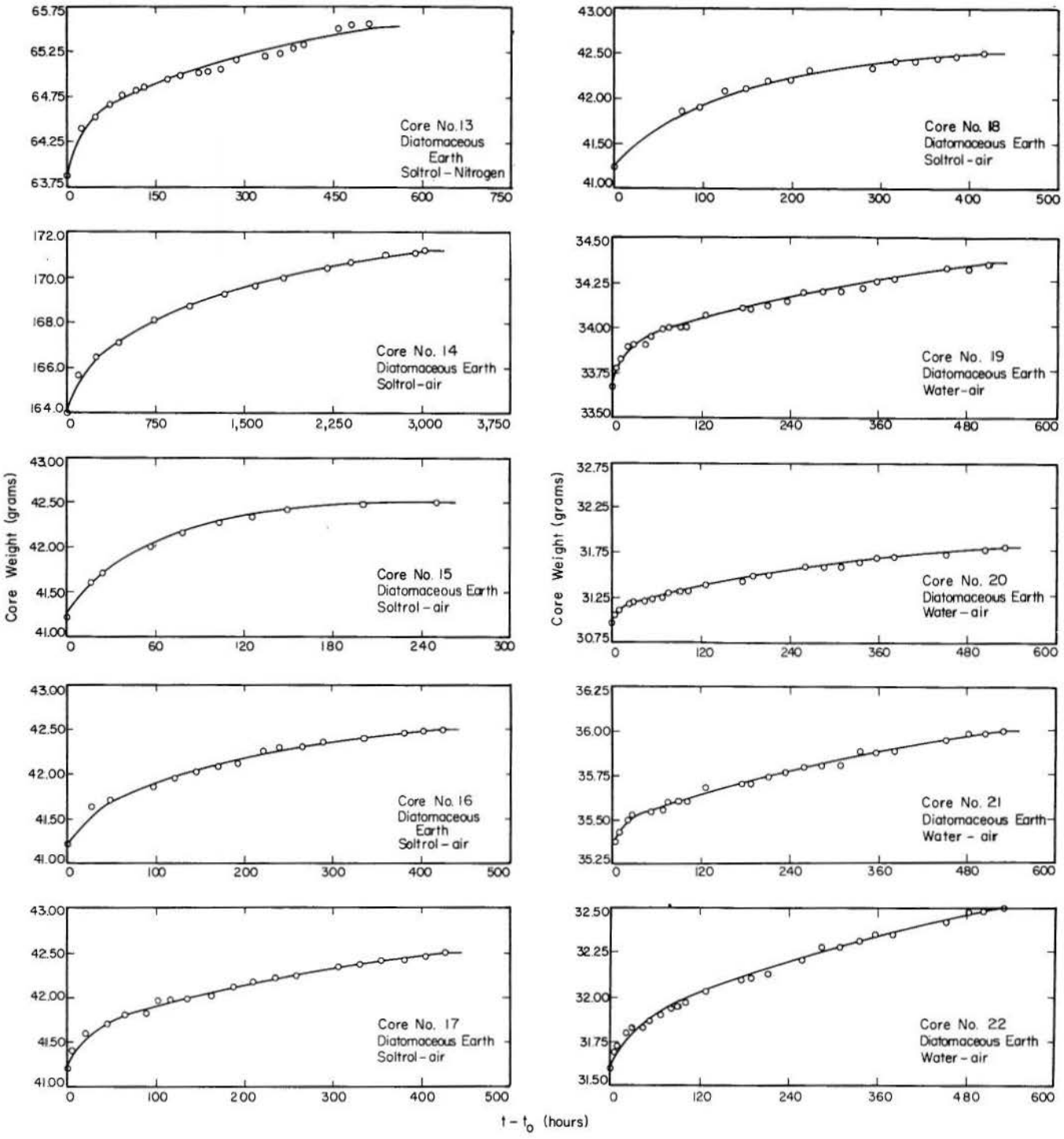

Figure 14. Core weight as a function of time - Continued

curves were plotted are given in Appendix A with related calculations. It can be observed from these curves that the samples all gain weight in a similar manner. Regardless of the material, the sample gains weight rapidly at the beginning of the measured time and the rate of gain decreases as time increases.

It was found that ambient pressure changes affected the liquid intake considerably. This result could be expected since the fluctuations in liquid pressure corresponds to changes in ambient pressure resulting in changes of pressure of the gaseous phase. These pressure changes of the gaseous phase cause volume changes in the gas pockets which are reflected in the weight of the core at any given time. For this reason, data were recorded only when the barometric pressure was in the range of 630.0 to 640.0 mm of mercury.

It is difficult to judge the zero time, that is, the time at which the imbibition process stops. Diffusion undoubtedly begins as soon as the wetting front enters the sample, but the entire gain in weight cannot be attributed to this until a few hours after the liquid first reaches the exterior face. During these few hours some gas is able to leave the sample by bulk flow. At larger times the data for gain in weight per unit area as a function of time can be represented closely by a straight line on a log-log plot. It was found that if a small value of time, t_o, was subtracted from the recorded times, all data points plotted along a straight line. Since t_o was always a time after the wetting front reached the exterior face, and at which one could reasonably expect the imbibition to be complete, the beginning of the diffusion process was defined as the time at which $t-t_o$ is zero. These data are presented in Figure 15. The lines through the data points were fit by a "least squares" method. The correlation coefficient exceeded 0.980 in every case. The lowest correlation coefficient obtained was that for core No. 15 which was prepared by the Bloomsburg method.

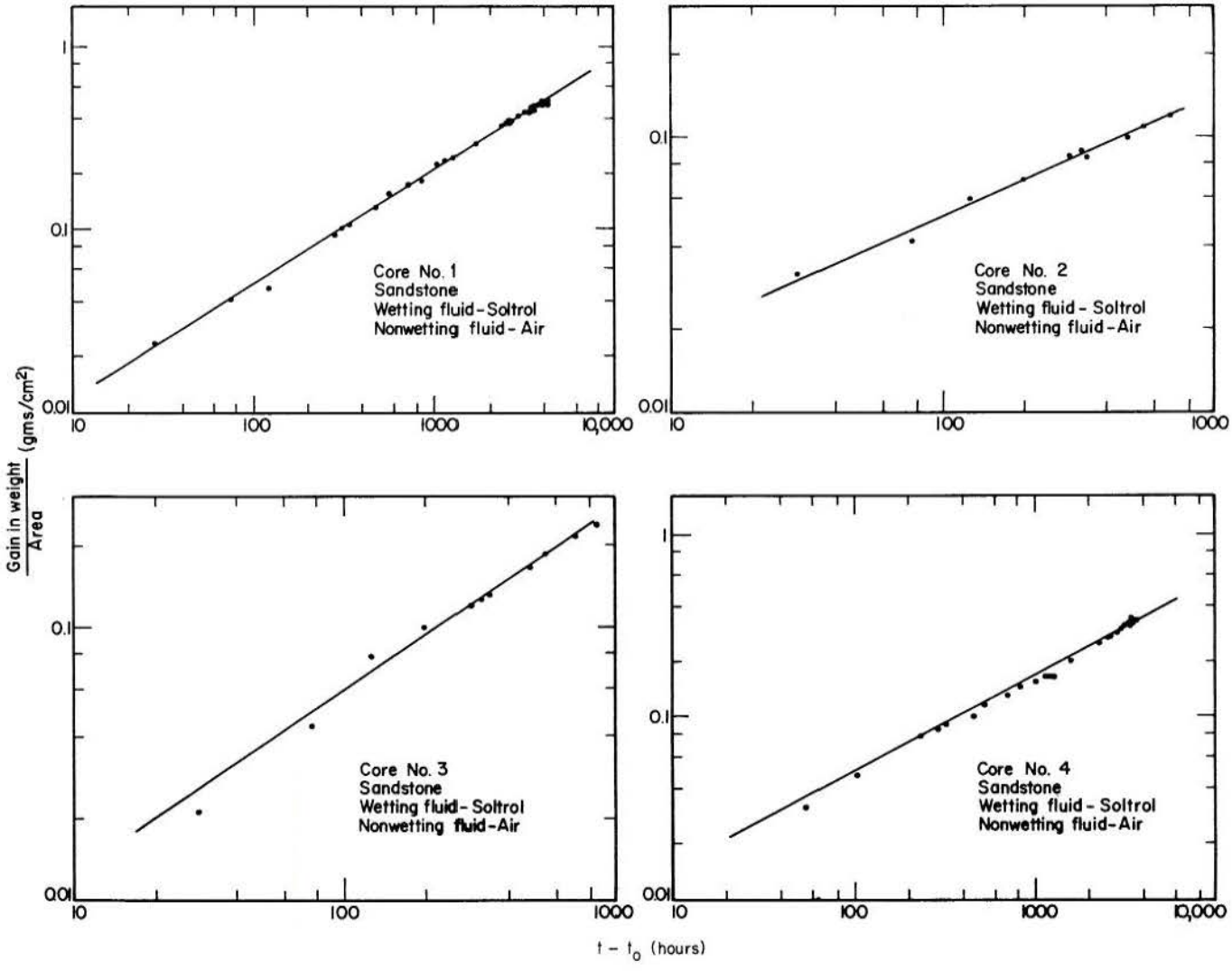

Figure 15. Gain in weight/area as a function of time

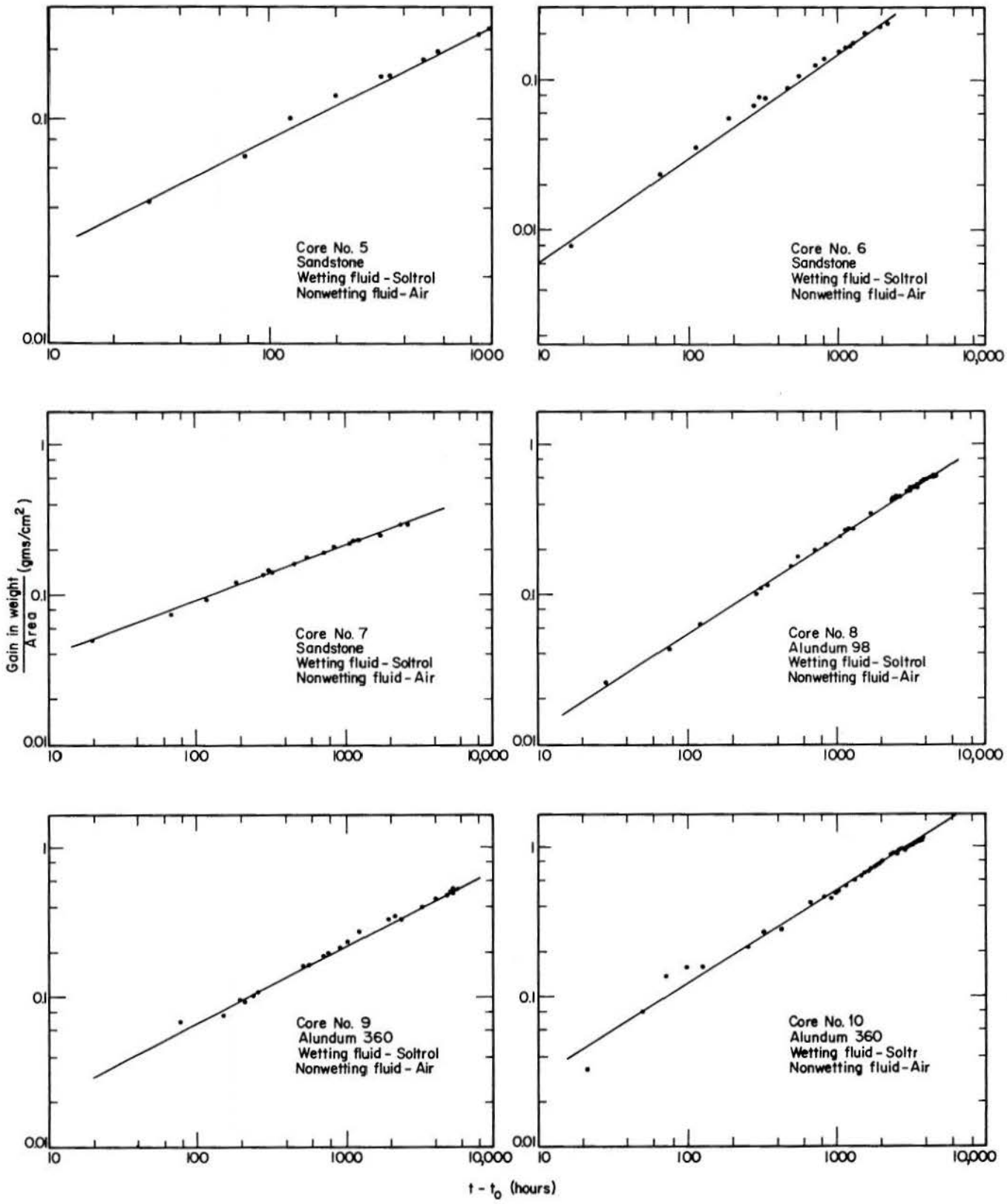

Figure 15. Gain in weight/area as a function of time - Continued

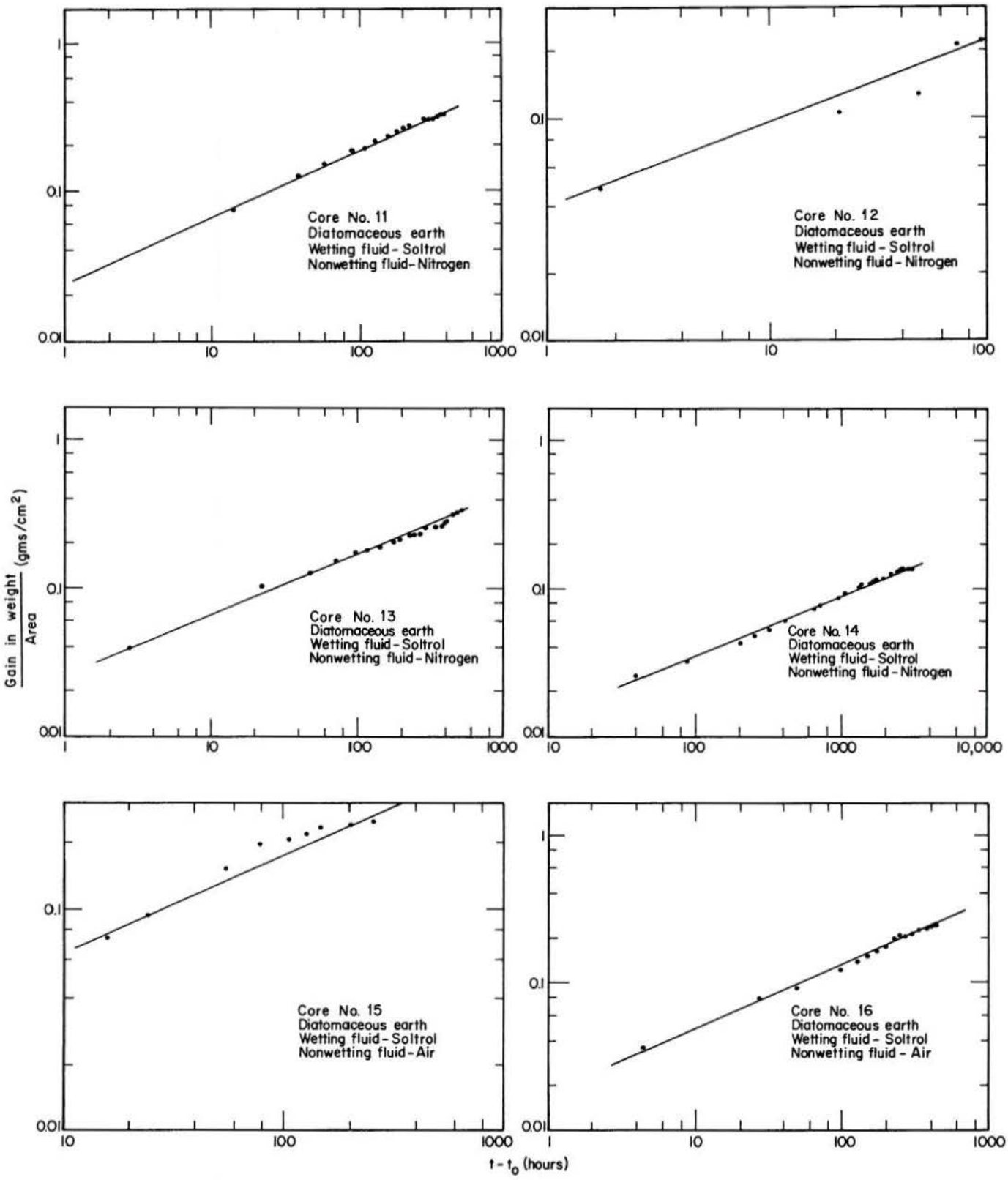

Figure 15. Gain in weight/area as a function of time - Continued

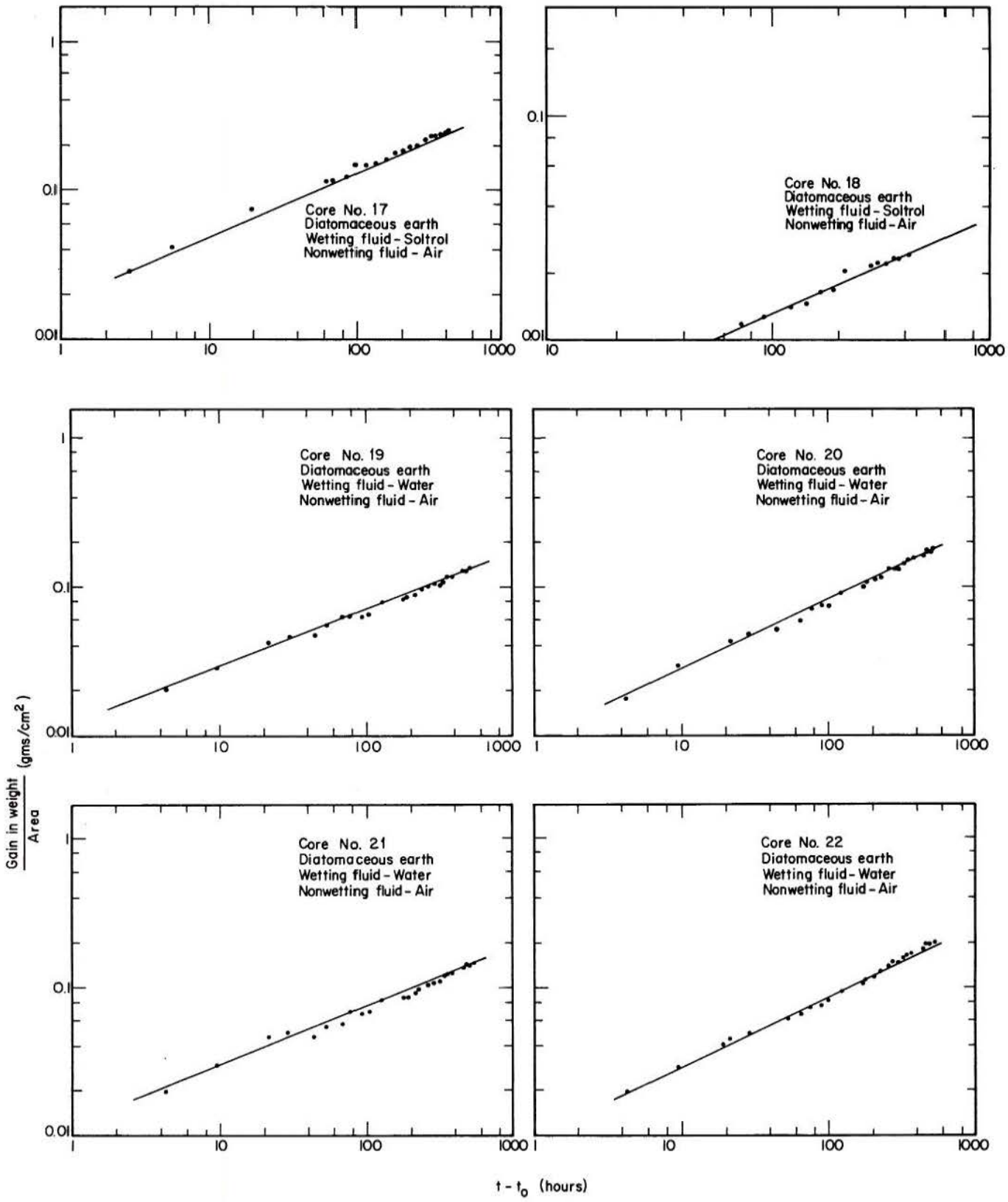

Figure 15. Gain in weight/area as a function of time - Continued

The equation of the straight line on log-log paper is

$$\frac{W - W_o}{A} = at^b \qquad (24)$$

where a and b are constants. This equation is of the same form as Equation (18), that is,

$$\frac{V_f}{V_{ao}} = \left[\frac{2C_o D_e}{(1-S_o)\phi L^2}\frac{\rho_\ell}{\rho_a}\right]^{\frac{1}{2}} t^{\frac{1}{2}} .$$

Equation 24 can be converted so as to have the same dependent variable on the left by dividing both sides by $(W_s - W_o)/A$. Equation (24) then becomes

$$\frac{V_f}{V_{ao}} = \frac{aA}{W_s - W_o} t^b . \qquad (25)$$

since

$$\frac{W - W_o}{W_s - W_o} = \frac{V_f}{V_{ao}} .$$

Another interesting result is found when the time variable is made dimensionless in Equation (25) by multiplying the right side by $t_s^{\frac{1}{2}}/t_s^{\frac{1}{2}}$. Equation (25) becomes

$$\frac{V_f}{V_{ao}} = \left[\frac{a\, t_s^{\,b}}{W_s}\right] t.^b \qquad (26)$$

where $t.$ signifies a dimensionless time. Since $V_f/V_{ao} = 1$ when $t = t_s$ or $t. = 1$, $a(t_s)^{\frac{1}{2}}/W_s$ must be equal to unity. The parameters of the above equations are given in Table 3. The value of D has been corrected for tortuosity by a factor of 2.0, since the effective coefficient of diffusion, D_e , in a porous medium is often considered to be D/T^2. It is obvious from the last column of Table 3 that the theoretical coefficient

$$\left[\frac{2C_o D_e}{(1-S_o)\phi T^2 L^2}\frac{\rho_\ell}{\rho_a}\right]^{\frac{1}{2}}$$

is not equal to the coefficient "a" obtained from the data.

In Appendix B, the same data are presented by plotting V_f/V_{ao} as a function of $(D_e t/L^2)^{\frac{1}{2}}$. This is the method used by Bloomsburg, which prescribes the exponent as $\frac{1}{2}$, and the variation is absorbed in the theoretical slope $[2C_o/(1-S_o)\phi(\rho_\ell/\rho_a)]^{\frac{1}{2}}$. Comparison of the actual slopes of these data to the theoretical slopes as given in Table B-1 indicate that neither Equation (3) nor Equation (18) adequately describe the process. Comparison of values of α given also in Table B-1, indicate a wide range of values for this constant. The constant α was calculated using Equation (13). Appendix C gives plots of V_f/V_{ao} as a function of dimensionless time.

The conclusion that neither Equation (3) or (18) adequately describe the process is understandable, considering the data obtained with the use of the gamma ray equipment. These data show that a sample gains in liquid content not only as a distinct front moving through the sample, but that the saturation increases with time throughout the sample. Figures 16 and 18 show the basis of this observation. These graphs are

TABLE 3. ACTUAL AND THEORETICAL SLOPES FOR GAIN IN WEIGHT AREA AS A FUNCTION OF TIME

Core No.	Equation (24) a	b	$\frac{W_s - W_o}{A}$	$\frac{aA}{W_s - W_o}$	Equation (18) $\left[\frac{2C_o D_e}{(1-S_o)\phi T^2 L^2}\frac{\rho_\ell}{\rho_a}\right]^{\frac{1}{2}}$	Equation (25) $\frac{a\, t_s^{\frac{1}{2}}}{W_s - W_o}$	$\frac{aA/W_s - W_o}{\left[\frac{2C_o D_e}{(1-S_o)\phi T^2 L^2}\frac{\rho_\ell}{\rho_a}\right]^{\frac{1}{2}}}$
1	0.0027	0.63	0.505	0.00535	0.000674	1.02	7.9
2	0.0075	0.43	0.120	0.0625	0.00182	1.00	34.3
3	0.0026	0.67	0.250	0.0104	0.00125	1.12	8.3
4	0.0050	0.50	0.334	0.0150	0.00139	0.94	10.8
5	0.0086	0.50	0.244	0.0352	0.00104	1.04	33.8
6	0.0015	0.67	0.237	0.00633	0.000990	1.05	6.4
7	0.0173	0.37	0.297	0.0582	0.000849	1.03	68.6
8	0.0027	0.68	0.631	0.00428	0.00165	1.05	2.6
9	0.0065	0.51	0.538	0.0121	0.000794	1.00	15.2
10	0.0075	0.61	1.622	0.00462	0.00249	0.97	1.9
11	0.0257	0.43	0.333	0.0772	0.00287	1.04	26.9
12	0.0398	0.36	0.332	0.120	0.00293	1.02	41.0
13	0.0282	0.39	0.339	0.0832	0.00292	0.95	28.5
14	0.0498	0.47	1.376	0.0362	0.00785	1.06	4.6
15	0.0231	0.45	0.245	0.0943	0.00341	1.16*	27.7
16	0.0189	0.43	0.245	0.0771	0.00341	1.02	22.6
17	0.0193	0.42	0.245	0.0788	0.00341	1.00	23.1
18	0.0114	0.43	0.245	0.0465	0.00341	1.03	13.6
19	0.0123	0.39	0.141	0.0872	0.00142	0.96	61.4
20	0.0098	0.47	0.193	0.0508	0.00123	0.96	41.3
21	0.0120	0.39	0.146	0.0822	0.00141	0.94	58.3
22	0.0095	0.48	0.199	0.0477	0.00123	0.95	38.8

*Bloomsburg Method

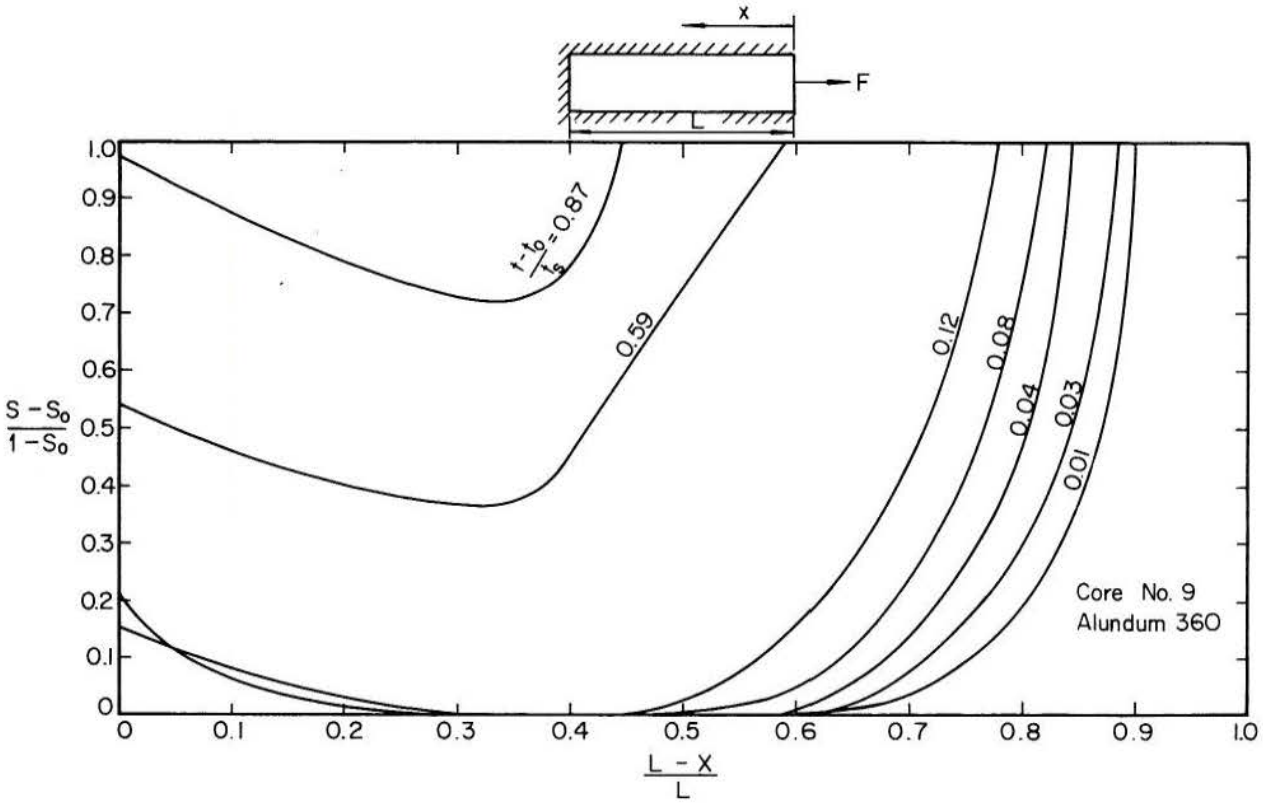

Figure 16. Normalized saturation as a function of normalized length and time

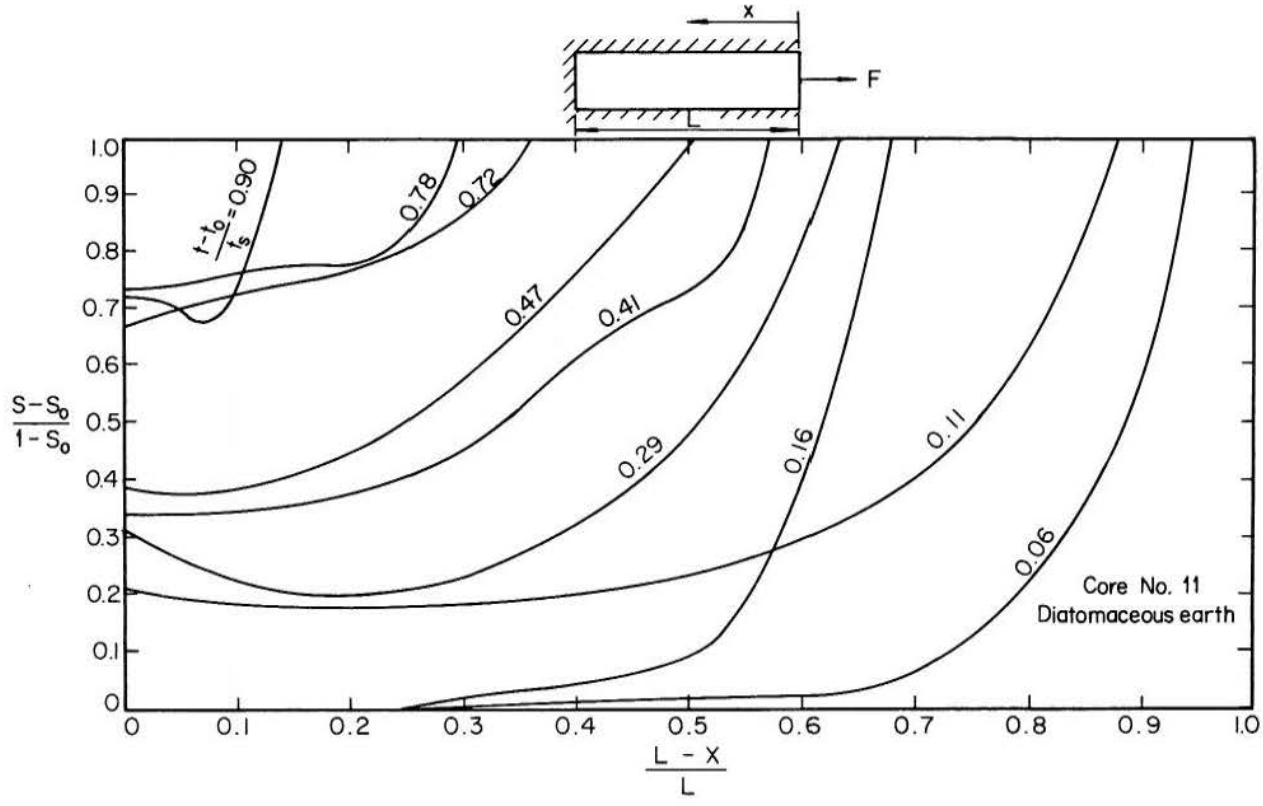

Figure 17. Normalized saturation as a function of normalized length and time

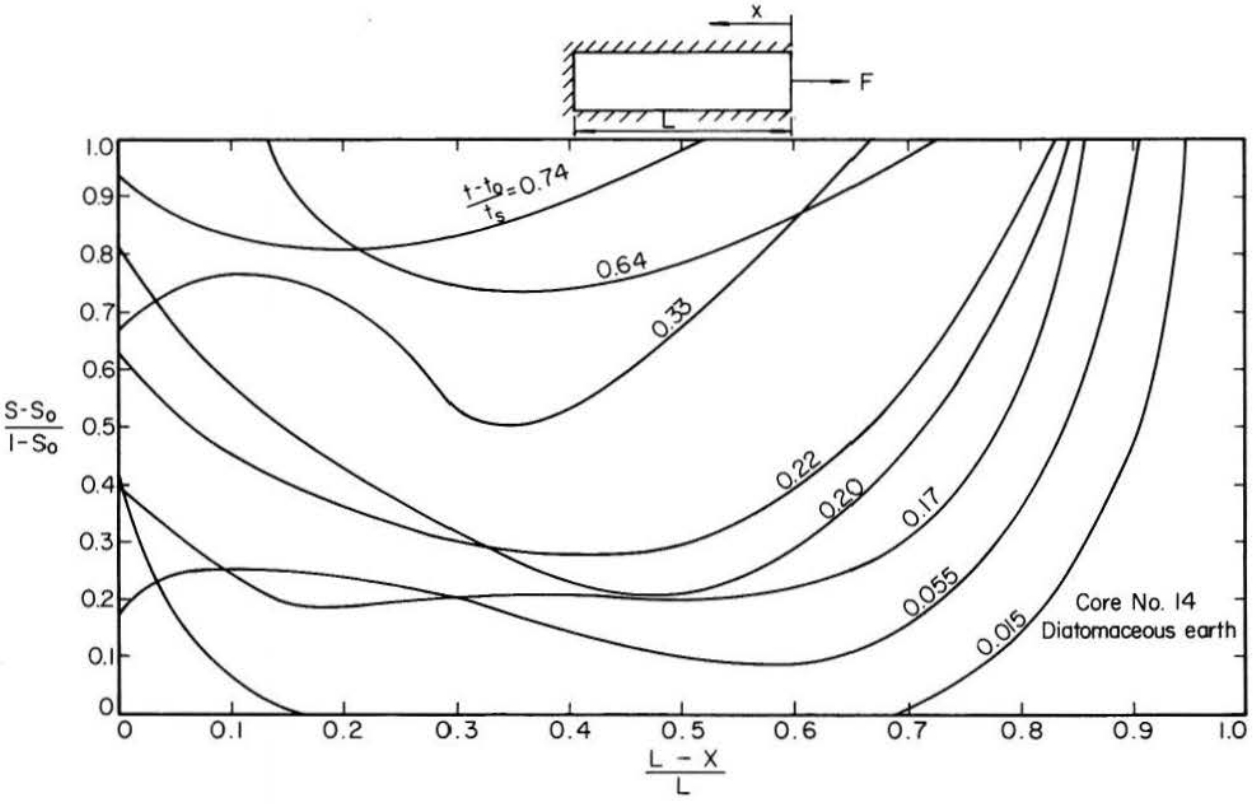

Figure 18. Normalized saturation as a function of normalized length and time

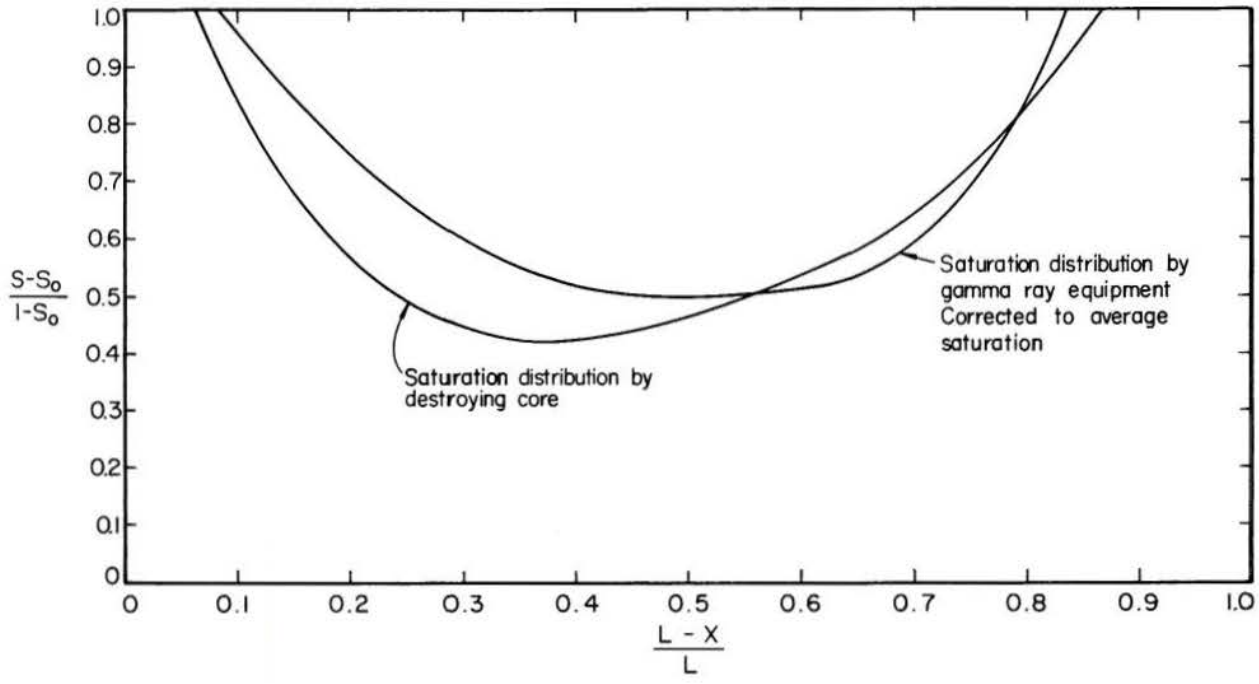

Figure 19. Comparison of saturation distribution obtained by gamma ray equipment and direct weighing of destroyed sample

plots of x/L as a function of $(S - S_o)/(1 - S_o)$ with $(t - t_o)/t_s$ as parameters. The data were normalized by dividing each variable by a characteristic dimension or the system. The data were fitted by a "least squares" method using a fifth degree polynomial. Furthermore, the curves were shifted vertically until the value of average saturation obtained by mechanical integration corresponded to the average saturation obtained by weighing the sample.

The shifting of the curves in a vertical direction (until the average saturation corresponds to a value obtained by weighing the sample) is based on the assumption that the gamma ray equipment gives a proper relative distribution of liquid in the sample, but not necessarily the correct liquid content at any point. Some confidence was gained in this procedure by allowing Core No. 10 to imbibe fluid in the usual manner for almost 4,000 hours. At this time, the liquid distribution was found by using the gamma ray equipment, and the sample weight was recorded. The average saturation was determined from the weight measurement, and the liquid distribution curve was adjusted vertically until the two average saturations corresponded. The sample, which was approximately 20 centimeters in length, was then cut into several pieces and the average saturation for each piece was found. By this method another liquid distribution curve was found. Figure 19 shows that the two curves indicate a similar distribution of liquid.

Several liquid distribution curves from Core Nos. 9, 11 and 14, corresponding to approximately equal normalized times, are given in Figure 20. These curves show that although the material, length, time for complete saturation and initial saturation vary considerably, the normalized data for equal normalized times are similar. This undoubtedly implies that most of the important variables have been taken into account in the normalizing procedure.

Considering the relationship

$$\frac{V_f}{V_{ao}} = \frac{S - S_o}{1 - S_o} ,$$

any of the curves in Figures 16 through 18 show that the volume of gas decreases with time throughout the partially saturated region. However, it is also obvious that a zone of full saturation exists, and it proceeds from the exterior face toward the interior as predicted by Bloomsburg.

It should be noted that, for certain times, as much as 50% of the gain in weight of the sample can be attributed to an increase in saturation in the partially saturated region. Considering the assumption in the theoretical development that the gas goes into solution only at the moving front, the fact that the theoretical and observed parameters do not correspond is not surprising.

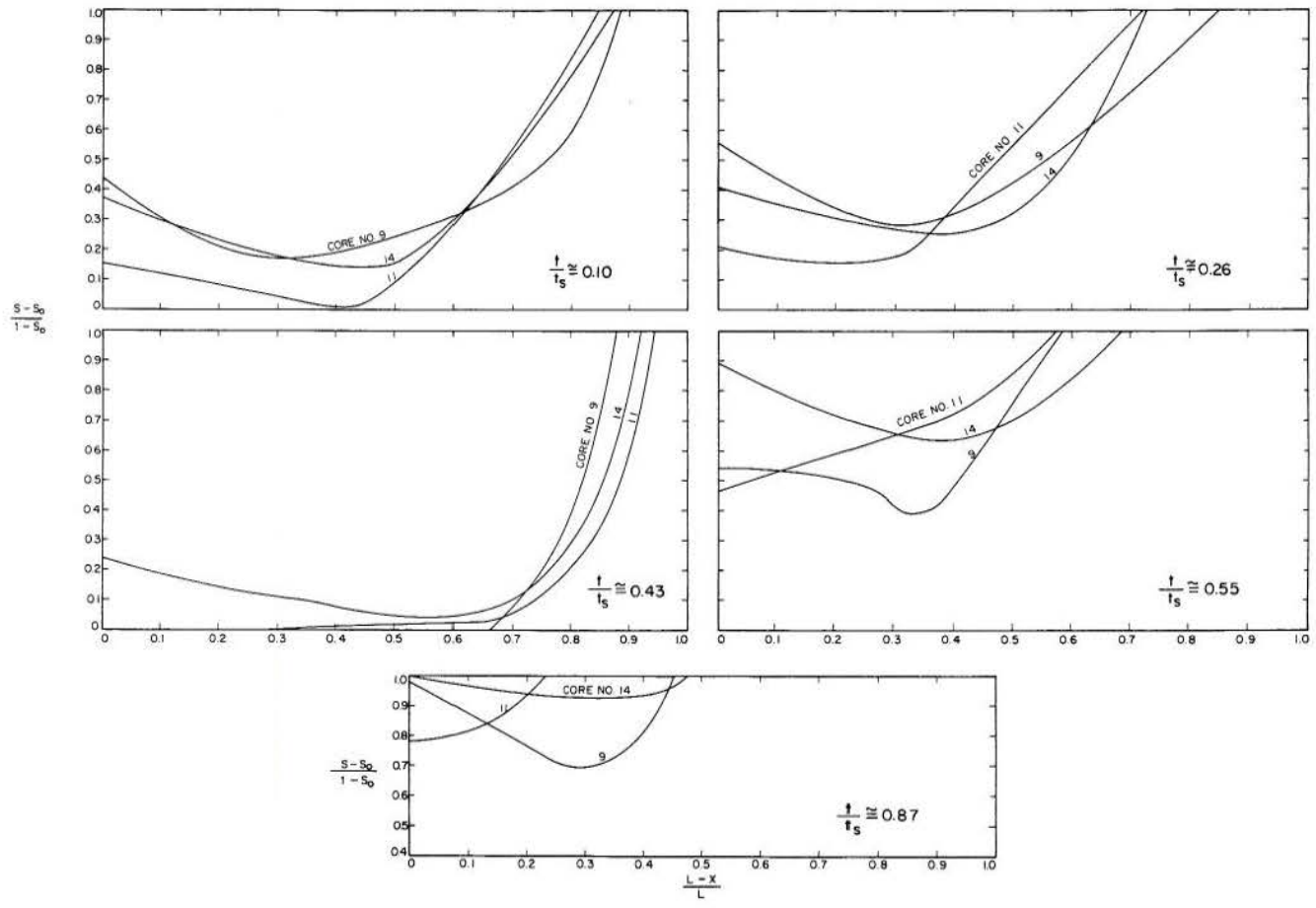

Figure 20. Normalized curve of saturation as a function of length for constant times

A standard statistical test in linear regression is a test that allows one to test the hypothesis that the slopes of two lines are not significantly different. The equations

$$y = \beta_i x + \alpha_i \ , \quad \text{where} \quad i = 1,2,3,\ldots,j-k,\ldots j \qquad (27)$$

for two or more straight lines, can be tested by use of a "student's t-distribution" to determine if the slopes are significantly different; that is, if

$$\beta_i = \beta_{j-k} \qquad (28)$$

where

$$k = 1,2,3,\ldots,j-1 \ .$$

The confidence interval of each β can be used. The confidence interval of β is

$$\beta = b \pm t_{0.01} \sqrt{\frac{s^2}{\Sigma(x-\bar{x})^2}} \qquad (29)$$

where b is the slope of the estimated line of regression, t is a tabulated value of the student's t-distribution with $(n-2)$ degrees of freedom, where n is the number of data points for a given line, and

$$\sqrt{\frac{s^2}{\Sigma(x-\bar{x})^2}}$$

is the standard deviation regression coefficient. If the confidence intervals of any two β's overlap, the two β's are not significantly different.

Table 4 gives the upper and lower bounds of the confidence interval of each regression line through the data of gain in weight/area as a function of time as presented in Figure 15. Comparison of confidence intervals in this table indicates that there is a significant difference at the 1% significance level between the two Alundum 360 cores, Core Nos. 9 and 10. However, excluding Core No. 13, all the diatomaceous earth cores, Nos. 11-18, inclusive, show no significant difference in the β_i's when Soltrol is the wetting fluid. When water was the wetting fluid used in diatomaceous earth, no significant difference was found between Core Nos. 19 and 21, and Core Nos. 20 and 22. However, Core Nos. 19 and 21 were significantly different from Core Nos. 20 and 22. These differences could be attributed to the less consistent wetting properties of water, or to nonhomogeneity of materials.

It is apparent that the slope, b, of cores of the same material are in the same range. Based on this observation, a graphical method of predicting the rate of diffusion of entrapped gas can be developed. Every core except No. 15, which was prepared by Bloomsburg's method, yielded data represented by a straight line on a log-log paper as shown in Figure 15. The fact that a straight line fits the data for every core indicates that extrapolation of the line is appropriate. Establishing the slope of the line with data corresponding to relatively short times removes the necessity of continuing the experiment for longer times.

This method was used in order to obtain the time of complete saturation, t_s, for Core Nos. 10 and 12. These samples were prepared in the usual manner. Data were collected and plotted until a sufficient number of points were obtained to establish the slope of the straight line. This line was extended until the gain in weight/area value corresponded to the saturated value. A corresponding time for complete saturation of the sample is obtained in this manner. This method is illustrated graphically in Figure 21. If the porosity, initial saturation and liquid density of the sample are known, the value of gain in weight/area

TABLE 4. STATISTICAL COMPARISON OF RESULTS

Core No.	n-2	$t_{0.01}$	Upper Bound β	b	Lower Bound β
1	35	2.44	0.644	0.632	0.620
2	8	2.90	0.480	0.431	0.382
3	10	2.76	0.738	0.672	0.606
4	28	2.47	0.531	0.501	0.471
5	9	2.82	0.536	0.497	0.458
6	16	2.58	0.712	0.673	0.634
7	17	2.57	0.382	0.367	0.352
8	35	2.44	0.658	0.648	0.638
9	23	2.50	0.530	0.512	0.494
10	38	2.43	0.636	0.607	0.578
11	15	2.60	0.447	0.434	0.421
12	4	3.75	0.529	0.364	0.199
13	18	2.55	0.411	0.391	0.371
14	20	2.53	0.435	0.417	0.399
15*	7	3.00	0.535	0.453	0.371
16	14	2.62	0.450	0.426	0.402
17	19	2.09	0.434	0.421	0.408
18	11	2.20	0.496	0.448	0.400
19	20	2.53	0.405	0.385	0.365
20	20	2.53	0.496	0.468	0.440
21	20	2.53	0.418	0.388	0.358
22	20	2.53	0.502	0.477	0.452

*Bloomsburg's Method

corresponding to that which would occur at full saturation can be calculated.

In Figure 22 the average curves for given times as obtained from Figure 20 are presented. Using the final time for complete saturation from Figure 21, the saturation distribution for a given sample can be estimated from Figure 18. At the present time, this graphical method gives the best available estimate of distribution of entrapped gas as a function of length and time.

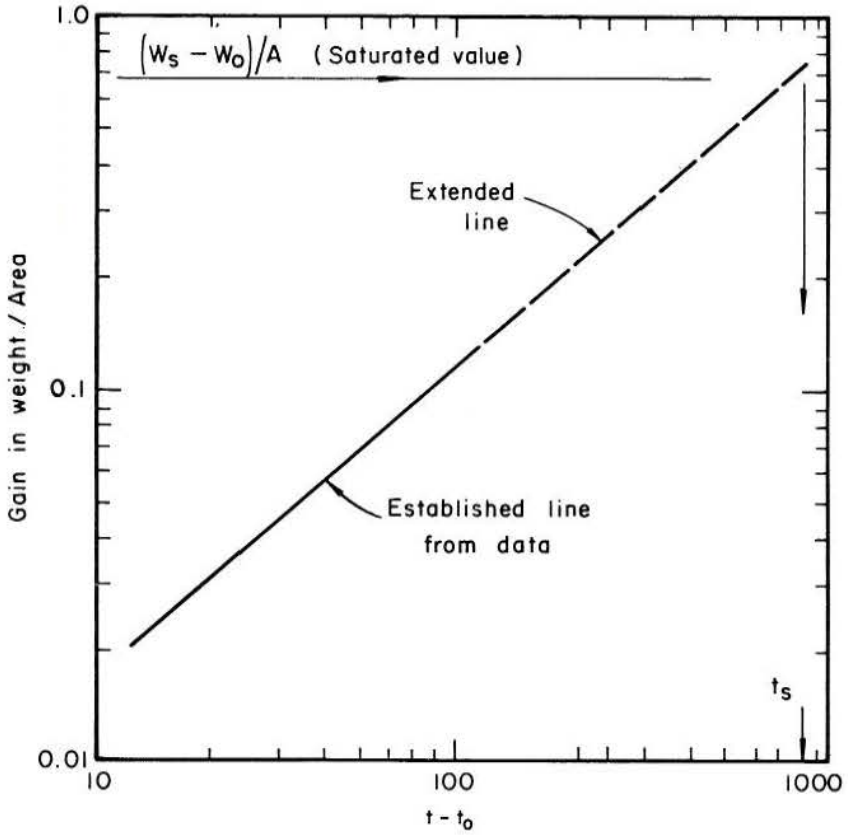

Figure 21. Graphical procedure for determination of time for complete saturation

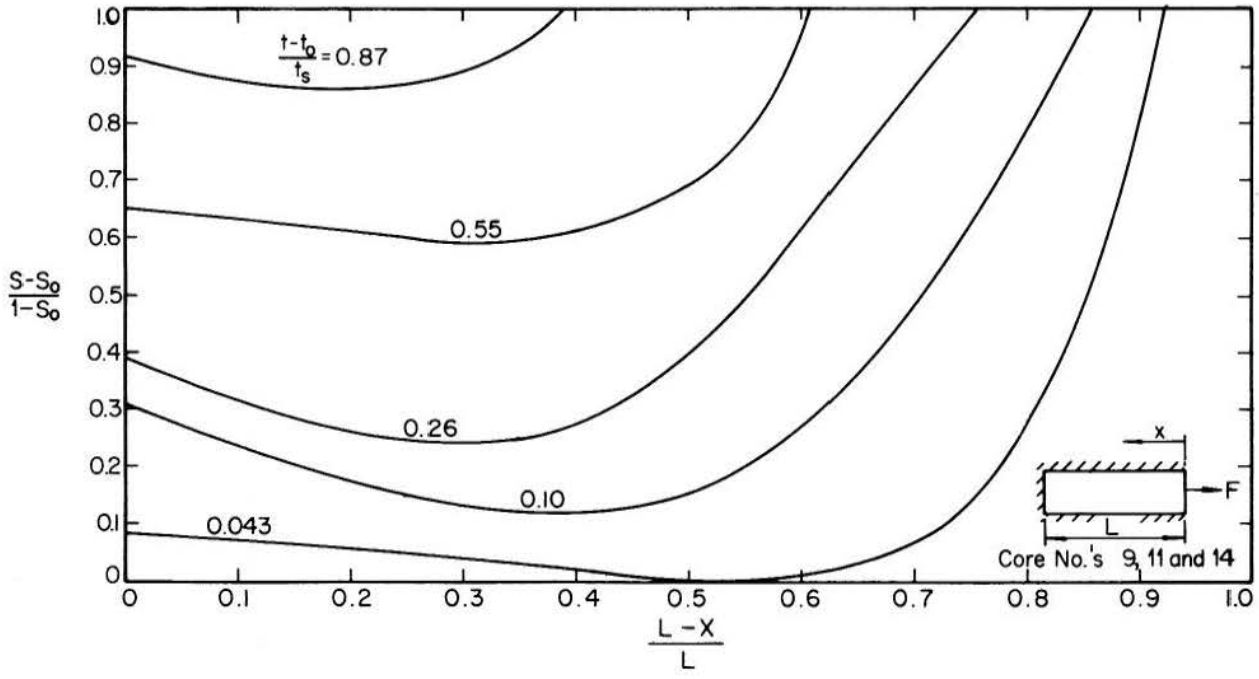

Figure 22. Average normalized data giving saturation as a function of length and time

CONCLUSIONS AND RECOMMENDATIONS

The experimental results of this study are consistent. In every core, regardless of the preparation method, the process proceeded in the same manner provided consistent boundary conditions were imposed. The consistency and reproducibility of these data generate confidence in the results. Based upon these results the data warrant the following conclusions:

1. A zone of complete saturation forms at the exterior face and moves continuously toward the interior as predicted by Bloomsburg.

2. Toward the interior from the saturated zone, some gain in weight occurs in the partially saturated region and the saturation in this region increases continuously. The rate of increase of saturation is greater near the saturated zone.

3. Any theoretical equation developed based on the assumption that air dissolved into the liquid only in the neighborhood of a well defined front of fully saturated medium cannot adequately describe the process of diffusion of entrapped gas.

4. The rate of diffusion of entrapped gas is greatest for materials with high bubbling pressures or fine grained materials. The fine grains are associated with small voids which confine entrapped air in pockets with small radii of curvature. This results in higher concentration of dissolved gas in the liquid.

5. The amount of gas initially entrapped is affected by the ambient pressure at the time of initial imbition.

6. Changes in barometric pressure affect the volume of gas entrapped in the medium at any time throughout the process.

7. The most practical method of describing the diffusion of entrapped gas from a porous medium at present is to extend experimental data of gain in weight/area as a function of time to the range of values which are of interest. The distribution of gas at various times is given as a function of normalized length and time.

The success of research to develop a theoretical equation to describe the diffusion of entrapped gas from a porous medium will depend on advances in the related areas. The knowledge of the shape of pockets of entrapped gas, the dependence of the dissolution of entrapped gas upon the surrounding concentration of gas in the liquid, and the development of a relationship between the volume of gas in the form of pockets and the mass of gas in these pockets must be extended. Progress in these areas will aid in formulating a source term which may allow the solution of the problem by the classical mathematical methods which usually give a solution to diffusion problems.

The experimental data of future studies should be collected with controlled ambient pressure. This would eliminate one variable from the system, or facilitate the study of the effect of this variable. With such controlled facilities, the factors affecting the initial quantity of entrapped gas may be determined.

The dissolution of entrapped gas, closest to the liquid supply, due to the gas concentration in that liquid being less than the concentration in the liquid already in the sample could occur in field processes. From this standpoint, this phenomenon should be studied as part of the problem.

BIBLIOGRAPHY

1. Adam, N. K. The physics and chemistry of surfaces: 3rd ed., Oxford University Press, 1941.

2. Barlow, E. J., and Langlois, W. E., Diffusion of gas from a liquid into an expanding bubble: IBM Journal of Research and Development, 6:329-337, July 1962.

3. Birkhoff, G., Marguilies, R. S., and Horning, W.A., Spherical bubble growth: Physics of Fluids, 1(3): 201-204, May-June 1958.

4. Bloomsburg, G. L., and Corey, A. T., Diffusion of entrapped air from porous media: Hydrology Paper No. 5, Colorado State University, Fort Collins, Colorado, 1964.

5. Brooks, R. H., and Corey, A. T., Hydraulic properties of porous media: Hydrology Paper No. 3., Colorado State University, March 1964.

6. Christiansen, J. E., Effect of entrapped air upon the permeability of soils: Soil Science, 58(5): 355-365, November 1944.

7. Churchill, R. V., Fourier series and boundary value problems: McGraw-Hill Book Company, 1963.

8. Corey, A. T., Diffusion of entrapped gas: Company Report, Gulf Research and Development Company, Pittsburg, Pa., 1952.

9. Davies, J. T., and Rideal, F. K., Interfacial phenomena: New York and London, Academic Press, 1961.

10. Dergarabedian, P., The rate of growth of vapor bubbles in superheated water: Jour. of Appl. Mech. 20(4):537-545, 1953.

11. Epstein, P. S., and Plesset, M. S., On the stability of gas bubbles in liquid-gas solutions: Jour. of Chemical Physics, 18 (11):1505-1509, November 1950.

12. Ferguson, A. H., Movement of soil water as inferred from moisture content measurements by gamma ray absorption: Ph.D. Thesis, Washington State University, Pullman, Washington, 1959.

13. Fox, F. E., and Herzfeld, K. F., Gas bubbles with organic skin as cavitation nuclei: Acoustical Society of America, Journal, 26(6):984-989, November 1954.

14. Gardescu, I. I., Behavior of gas bubbles in capillary spaces: Amer. Inst. of Mining Engr., Transactions, 86:351-370, 1930.

15. Gupta, R. P., and Swartzendruber, D., Entrapped air content and hydraulic conductivity of quartz sand during prolonged liquid flow: Soil Science Soc. of Amer. Proc., 28(1): 9-12, January-February 1964.

16. Hawke, J. G., and Parts, A. G., A coefficient to characterize gaseous diffusion through monolayers at the air/water interface: Journal of Colloid Science, 19:448-456, 1964.

17. Levenspiel, O., Collapse of stream bubbles in water: Industrial and Engineering Chemistry, 51:787-790, 1959.

18. Liebermann, L., Air bubbles in water: Jour. of Applied Physics, 28(2):205-211, February 1957.

19. Ma, J. T. S., and Wang, P. K. C., Effect of initial air content on the dynamics of bubbles in liquids: IBM Jour. of Research and Development, 6(4): 472-474, October 1962.

20. Orlob, G. T., and Radhakrishna, G. N., The effects of entrapped gases on the hydraulic characteristics of porous media: American Geophysical Union, Transactions, 39(4):648-659, Aurust 1958.

21. Philip, J. R., The theory of infiltration: I the infiltration equation and its solutions: Soil Science, 83(5):345-357, May 1957.

22. Powers, W. L., Soil water movement as affected by confined air: Jour. of Agricultural Research, 49 (12):1125-1133, 1934.

23. Reinhart, K. G., and Taylor, R. E., Infiltration and available water storage capacity in the soil: Trans. Amer. Geophys. Union, XXXV:791-795, October 1954.

24. Rouse, H., Elementary mechanics of fluids: New York, John Wiley and Sons, Inc., 1946.

25. Wyllie, M. R. J., and Spangler, M. B., Application of electrical resistivity measurements to the problem of fluid flow in porous media: Bulletin of the American Association of Petroleum Geologists, Vol. 36, No. 2, February 1952.

26. Zimmerman, B. G., Determining entrapped air in capillary soils: Engineering News Record, 117(6): 186-187, August 6, 1936.

APPENDIX A

EXPERIMENTAL DATA AND CALCULATIONS

TABLE A-1. EXPERIMENTAL DATA AND CALCULATIONS

Time $t-t_o$ (hrs)	$\frac{t-t_o}{t_s}$ (dimensionless)	Weight (grams)	Weight gain per unit area above W_o (grams/cm^2)	$\frac{V_f}{V_{ao}}$ (dimensionless)	Average saturation S (dimensionless)
			CORE NO. 1		
0.0	0.00000	61.29	0.0000	0.0000	0.637
28.5	0.00676	61.41	0.0237	0.0469	0.654
76.0	0.0180	61.50	0.0415	0.0822	0.667
124.0	0.0294	61.53	0.0474	0.0939	0.671
289.0	0.0685	61.75	0.0908	0.180	0.702
316.0	0.0750	61.80	0.100	0.198	0.709
340.0	0.0807	61.81	0.102	0.202	0.711
480.0	0.114	61.95	0.130	0.256	0.730
557.0	0.132	62.08	0.156	0.309	0.749
726.0	0.172	62.19	0.177	0.350	0.765
850.0	0.202	62.26	0.181	0.358	0.774
1059.0	0.251	62.43	0.225	0.446	0.799
1178.0	0.280	62.48	0.235	0.465	0.806
1227.0	0.291	62.50	0.238	0.471	0.809
1298.0	0.308	62.51	0.240	0.475	0.810
1683.0	0.399	62.76	0.290	0.574	0.845
2355.0	0.559	63.15	0.367	0.727	0.901
2403.0	0.570	63.18	0.373	0.739	0.905
2570.0	0.610	63.24	0.385	0.762	0.913
2642.0	0.627	63.28	0.393	0.778	0.919
2690.0	0.638	63.28	0.393	0.778	0.919
2979.0	0.707	63.40	0.416	0.824	0.936
3146.5	0.747	63.49	0.434	0.859	0.949
3194.0	0.758	63.50	0.436	0.863	0.950
3315.0	0.787	63.52	0.440	0.871	0.953
3362.5	0.798	63.57	0.450	0.891	0.960
3412.0	0.810	63.60	0.455	0.901	0.965
3483.5	0.827	63.60	0.455	0.901	0.965
3530.0	0.838	63.62	0.460	0.911	0.967
3583.0	0.850	63.68	0.471	0.933	0.976
3698.0	0.878	63.68	0.471	0.933	0.976
3795.0	0.901	63.70	0.475	0.941	0.979
3870.0	0.919	63.73	0.481	0.952	0.983
3915.0	0.929	63.75	0.485	0.960	0.986
3963.0	0.941	63.77	0.489	0.968	0.987
4063.0	0.964	63.80	0.495	0.980	0.993
4130.0	0.980	63.82	0.499	0.988	0.996
4213.0	1.000	63.85	0.505	1.000	1.000
			CORE NO. 2		
0.0	0.0000	53.80	0.0000	0.000	0.810
28.5	0.0417	53.96	0.0318	0.265	0.860
76.0	0.111	54.01	0.0418	0.348	0.876
124.0	0.185	54.10	0.0597	0.497	0.905
196.0	0.287	54.15	0.0679	0.581	0.920
289.0	0.423	54.22	0.0836	0.697	0.943
316.0	0.463	54.24	0.0876	0.730	0.949
340.0	0.498	54.22	0.0836	0.697	0.943
480.0	0.703	54.30	0.100	0.833	0.968
557.0	0.816	54.37	0.114	0.950	0.990
683.0	1.000	54.40	0.120	1.000	1.000

TABLE A-1. EXPERIMENTAL DATA AND CALCULATIONS - Continued

Time $t-t_o$ (hrs)	$\frac{t-t_o}{t_s}$ (dimensionless)	Weight (grams)	Weight gain per unit area above W_o (grams/cm^2)	$\frac{V_f}{V_{ao}}$ (dimensionless)	Average saturation S (dimensionless)
			CORE NO. 3		
0.0	0.0000	50.51	0.0000	0.0000	0.674
28.5	0.0269	50.62	0.0221	0.0884	0.701
76.0	0.0718	50.73	0.0441	0.176	0.730
124.0	0.117	50.90	0.0782	0.313	0.774
196.0	0.181	51.01	0.100	0.400	0.803
289.0	0.273	51.11	0.120	0.480	0.829
316.0	0.298	51.15	0.128	0.512	0.839
340.0	0.321	51.16	0.130	0.520	0.842
480.0	0.453	51.33	0.164	0.656	0.886
557.0	0.526	51.44	0.186	0.744	0.914
726.0	0.686	51.57	0.212	0.848	0.948
850.0	0.803	51.69	0.236	0.944	0.979
1059.0	1.000	51.76	0.250	1.000	1.000
			CORE NO. 4		
0.0	0.00000	65.95	0.0000	0.0000	0.474
7.5	0.00201	66.05	0.0199	0.0596	0.505
55.0	0.0148	66.11	0.0318	0.0952	0.523
103.0	0.0277	66.19	0.0478	0.143	0.548
268.0	0.0451	66.33	0.0756	0.226	0.592
295.0	0.0792	66.36	0.0816	0.244	0.601
319.0	0.0856	66.39	0.0876	0.262	0.611
459.0	0.123	66.43	0.0955	0.286	0.623
536.0	0.144	66.52	0.113	0.338	0.651
705.0	0.189	66.60	0.128	0.383	0.676
829.0	0.223	66.67	0.142	0.425	0.698
1038.0	0.279	66.73	0.153	0.458	0.717
1157.0	0.311	66.77	0.162	0.485	0.729
1206.0	0.324	66.80	0.168	0.503	0.738
1277.0	0.343	66.80	0.168	0.503	0.738
1662.0	0.446	66.96	0.200	0.599	0.788
2334.0	0.627	67.19	0.245	0.734	0.860
2382.0	0.639	67.21	0.249	0.746	0.866
2549.0	0.684	67.28	0.263	0.787	0.888
2669.0	0.716	67.30	0.267	0.799	0.894
2958.0	0.794	67.40	0.286	0.856	0.925
3125.0	0.839	67.43	0.292	0.874	0.935
3173.0	0.852	67.48	0.302	0.904	0.950
3294.0	0.884	67.49	0.304	0.910	0.953
3341.0	0.897	67.52	0.310	0.928	0.963
3391.0	0.910	67.57	0.320	0.958	0.978
3461.0	0.929	67.56	0.318	0.952	0.975
3509.0	0.942	67.56	0.318	0.952	0.975
3562.0	0.956	67.62	0.330	0.988	0.994
3677.0	0.987	67.60	0.326	0.976	0.988
3725.0	1.000	67.64	0.334	1.000	1.000
			CORE NO. 5		
0.0	0.0000	47.79	0.0000	0.000	0.736
28.5	0.0303	48.00	0.04351	0.178	0.782
76.0	0.0808	48.12	0.0683	0.280	0.809
124.0	0.132	48.27	0.0994	0.407	0.843
196.0	0.208	48.40	0.126	0.516	0.873
289.0	0.307	48.49	0.145	0.594	0.893
316.0	0.336	48.53	0.153	0.627	0.902
340.0	0.361	48.55	0.157	0.643	0.907
480.0	0.510	48.67	0.182	0.746	0.934
557.0	0.592	48.74	0.197	0.807	0.950
850.0	0.903	48.91	0.234	0.959	0.991
941.0	1.000	48.96	0.244	1.000	1.000

TABLE A-1. EXPERIMENTAL DATA AND CALCULATIONS - Continued

Time $t-t_o$ (hrs)	$\frac{t-t_o}{t_s}$ (dimensionless)	Weight (grams)	Weight gain per unit area above W_o (grams/cm^2)	$\frac{V_f}{V_{ao}}$ (dimensionless)	Average saturation S (dimensionless)
			CORE NO. 6		
0.0	0.00000	54.67	0.00000	0.0000	0.472
16.5	0.00762	54.71	0.00790	0.0333	0.491
64.0	0.0296	54.79	0.0237	0.100	0.526
112.0	0.0517	54.85	0.0355	0.150	0.553
184.0	0.0850	54.95	0.0553	0.233	0.596
277.0	0.128	55.00	0.0652	0.275	0.618
304.0	0.140	55.06	0.0770	0.325	0.645
328.0	0.151	55.05	0.750	0.316	0.640
468.0	0.216	55.12	0.0888	0.377	0.667
545.0	0.252	55.22	0.107	0.451	0.711
714.0	0.330	55.30	0.123	0.519	0.746
838.0	0.387	55.38	0.138	0.582	0.781
1047.0	0.484	55.45	0.152	0.641	0.811
1166.0	0.539	55.49	0.160	0.675	0.829
1215.0	0.561	55.52	0.166	0.700	0.842
1286.0	0.594	55.55	0.172	0.726	0.855
1671.0	0.772	55.70	0.202	0.852	0.921
1970.0	0.910	55.80	0.221	0.932	0.965
2165.0	1.000	55.88	0.237	1.000	1.000
			CORE NO. 7		
0.0	0.00000	57.52	0.0000	0.000	0.477
19.5	0.00760	57.78	0.0513	0.175	0.568
67.0	0.0262	57.90	0.0750	0.253	0.610
115.0	0.0449	58.00	0.0948	0.320	0.645
187.0	0.0730	58.15	0.125	0.421	0.697
280.0	0.109	58.20	0.135	0.455	0.714
305.0	0.119	58.26	0.147	0.495	0.735
331.0	0.129	58.24	0.143	0.481	0.728
471.0	0.184	58.35	0.164	0.552	0.767
548.0	0.214	58.43	0.180	0.606	0.794
717.0	0.280	58.50	0.194	0.653	0.819
841.0	0.328	58.58	0.210	0.707	0.847
1050.0	0.410	58.64	0.222	0.747	0.868
1169.0	0.456	58.68	0.230	0.774	0.882
1218.0	0.476	58.70	0.234	0.788	0.889
1289.0	0.503	58.71	0.236	0.795	0.892
1674.0	0.654	58.82	0.257	0.865	0.930
2346.0	0.916	59.00	0.293	0.987	0.993
2394.0	0.935	59.00	0.293	0.987	0.993
2561.0	1.000	59.02	0.297	1.000	1.000
			CORE NO. 8		
0.0	0.00000	86.75	0.0000	0.0000	0.637
28.5	0.00606	86.90	0.0258	0.0412	0.631
76.0	0.0162	87.00	0.0430	0.0681	0.656
124.0	0.0264	87.11	0.0620	0.0983	0.666
289.0	0.0615	87.33	0.100	0.158	0.688
316.0	0.0672	87.39	0.110	0.174	0.694
340.0	0.0723	87.41	0.115	0.182	0.697
480.0	0.102	87.61	0.150	0.238	0.716
557.0	0.118	87.76	0.175	0.277	0.731
726.0	0.154	87.88	0.196	0.311	0.743
850.0	0.181	88.00	0.217	0.344	0.754
1059.0	0.225	88.19	0.246	0.390	0.771
1178.0	0.251	88.29	0.263	0.417	0.781
1227.0	0.261	88.37	0.277	0.439	0.789
1298.0	0.276	88.38	0.279	0.442	0.790
1683.0	0.358	88.65	0.342	0.542	0.826
2355.0	0.501	89.17	0.432	0.685	0.877
2403.0	0.511	89.23	0.442	0.700	0.883
2570.0	0.547	89.28	0.450	0.713	0.887
2690.0	0.572	89.34	0.461	0.731	0.893

TABLE A-1. EXPERIMENTAL DATA AND CALCULATIONS - Continued

Time $t-t_o$ (hrs)	$\frac{t-t_o}{t_s}$ (dimensionless)	Weight (grams)	Weight gain per unit area above W_o (grams/cm^2)	$\frac{V_f}{V_{ao}}$ (dimensionless)	Average saturation S (dimensionless)
			CORE NO. 8 - Continued		
2979.0	0.634	89.53	0.494	0.783	0.912
3146.5	0.669	89.61	0.508	0.805	0.920
3194.0	0.679	89.68	0.520	0.824	0.927
3315.0	0.705	89.72	0.526	0.834	0.931
3362.5	0.715	89.78	0.537	0.851	0.936
3412.0	0.726	89.82	0.544	0.862	0.940
3482.5	0.741	89.78	0.537	0.851	0.936
3530.0	0.751	89.82	0.544	0.862	0.940
3583.0	0.762	89.88	0.554	0.878	0.946
3698.0	0.787	89.92	0.561	0.889	0.950
3870.0	0.823	90.03	0.580	0.919	0.961
4063.0	0.864	90.15	0.601	0.952	0.973
4274.0	0.909	90.20	0.609	0.965	0.977
4448.0	0.946	90.27	0.615	0.975	0.984
4496.0	0.956	90.30	0.618	0.979	0.987
4541.0	0.966	90.33	0.621	0.984	0.990
4613.0	0.981	90.36	0.624	0.989	0.993
4701.0	1.000	90.43	0.631	1.000	1.000
			CORE NO. 9		
0.0	0.0000	97.82	0.0000	0.000	0.694
78.8	0.0139	98.22	0.0684	0.126	0.734
150.3	0.0265	98.27	0.0769	0.143	0.739
198.5	0.0350	98.37	0.0940	0.175	0.749
210.2	0.0371	98.37	0.0940	0.175	0.749
241.5	0.0426	98.42	0.103	0.191	0.754
269.5	0.0476	98.45	0.108	0.201	0.757
527.5	0.0931	98.75	0.159	0.296	0.786
576.3	0.102	98.78	0.164	0.305	0.789
700.5	0.124	98.92	0.188	0.349	0.803
773.0	0.136	98.97	0.197	0.366	0.807
925.0	0.163	99.07	0.217	0.403	0.819
1021.0	0.180	99.18	0.236	0.439	0.830
1240.0	0.219	99.41	0.272	0.506	0.850
1967.0	0.347	99.73	0.327	0.608	0.881
2187.0	0.386	99.85	0.347	0.645	0.893
2355.0	0.416	99.80	0.339	0.630	0.888
3315.0	0.585	100.16	0.400	0.743	0.923
4155.0	0.733	100.47	0.453	0.842	0.953
4659.5	0.822	100.58	0.472	0.877	0.964
4827.0	0.852	100.65	0.484	0.900	0.971
5019.0	0.886	100.75	0.501	0.931	0.981
5307.0	0.936	100.81	0.511	0.950	0.986
5475.0	0.966	100.91	0.528	0.981	0.990
5619.0	0.992	100.95	0.535	0.994	0.994
5667.0	1.000	100.97	0.538	1.000	1.000
			CORE NO. 10		
0.0	0.000	318.54	0.000	0.0000	0.741
70.0	0.0105	319.34	0.137	0.0845	0.763
97.0	0.0145	319.42	0.152	0.0937	0.765
122.0	0.0183	319.43	0.153	0.0943	0.765
253.0	0.0379	319.75	0.209	0.129	0.774
324.0	0.0485	320.04	0.259	0.160	0.782
426.0	0.0638	320.12	0.272	0.168	0.784
661.0	0.0989	320.90	0.407	0.251	0.806
828.0	0.124	321.16	0.452	0.279	0.813
924.0	0.138	321.08	0.438	0.270	0.811
996.0	0.149	321.29	0.474	0.292	0.816
1044.0	0.156	321.40	0.493	0.304	0.819
1164.0	0.174	321.66	0.538	0.332	0.827
1333.0	0.200	321.95	0.588	0.363	0.835
1500.5	0.225	322.17	0.626	0.386	0.841

TABLE A-1. EXPERIMENTAL DATA AND CALCULATIONS - Continued

Time $t-t_o$ (hrs)	$\frac{t-t_o}{t_o}$ (dimensionless)	Weight (grams)	Weight gain per unit area above W_o (grams/cm^2)	$\frac{V_f}{V_{ao}}$ (dimensionless)	Average saturation S (dimensionless)
		CORE NO. 10 - Continued			
1548.0	0.232	322.32	0.652	0.402	0.845
1669.0	0.250	322.43	0.671	0.414	0.848
1716.5	0.257	322.59	0.698	0.430	0.852
1766.0	0.264	322.57	0.695	0.428	0.852
1836.5	0.275	322.69	0.716	0.441	0.855
1884.0	0.282	322.74	0.724	0.446	0.856
1937.0	0.290	322.90	0.752	0.464	0.861
2052.0	0.307	323.05	0.778	0.480	0.862
2389.0	0.358	323.50	0.855	0.527	0.877
2489.0	0.373	323.59	0.871	0.537	0.880
2556.0	0.383	323.60	0.872	0.538	0.880
2700.0	0.404	323.88	0.921	0.568	0.888
2724.0	0.408	323.91	0.925	0.570	0.889
2748.0	0.411	324.04	0.927	0.572	0.892
2922.0	0.437	324.10	0.938	0.578	0.894
3180.0	0.476	324.31	0.974	0.600	0.900
3234.0	0.484	324.40	0.989	0.610	0.903
3505.0	0.525	324.70	1.041	0.642	0.910
3597.0	0.538	324.81	1.060	0.654	0.913
3666.0	0.549	324.85	1.067	0.658	0.914
3830.0	0.573	324.95	1.100	0.678	0.916
3899.0	0.584	325.03	1.119	0.690	0.919
3975.0	0.595	325.18	1.145	0.706	0.924
3997.0	0.598	325.20	1.148	0.708	0.924
6681.0*	1.000	327.95*	1.622*	1.000	1.000
		CORE NO. 11			
0.0	0.00000	63.89**	0.0000	0.0000	0.897
0.8	0.00202	64.01**	0.0239	0.0751	0.908
14.6	0.0370	64.27**	0.0756	0.231	0.924
40.1	0.101	64.53**	0.128	0.384	0.939
61.1	0.155	64.66**	0.154	0.462	0.947
91.1	0.231	64.81**	0.184	0.553	0.956
112.1	0.284	64.88**	0.198	0.595	0.960
137.6	0.348	65.00**	0.222	0.667	0.967
160.1	0.405	65.08**	0.238	0.715	0.972
184.1	0.466	65.14**	0.250	0.751	0.975
208.1	0.527	65.22**	0.266	0.799	0.980
227.1	0.575	65.28**	0.278	0.835	0.983
280.1	0.709	65.41**	0.304	0.913	0.991
307.1	0.777	65.44**	0.309	0.928	0.993
328.1	0.830	65.47**	0.315	0.946	0.995
351.1	0.889	65.50**	0.321	0.964	0.996
376.1	0.952	65.54**	0.329	0.988	0.999
395.1	1.000	65.56**	0.333	1.000	1.000
		CORE NO. 12			
0.0	0.00000	65.47	0.0000	0.000	0.901
1.0	0.00277	65.69	0.0438	0.132	0.914
1.8	0.00499	65.71	0.0478	0.144	0.916
21.5	0.0596	66.00	0.105	0.316	0.933
50.5	0.140	66.12	0.129	0.358	0.940
70.3	0.195	66.58	0.221	0.666	0.967
95.3	0.264	66.70	0.245	0.738	0.974
360.6*	1.000	67.14	0.332*	1.000	1.000

*Calculated values
**Calculated weight from calibrated input tube

TABLE A-1. EXPERIMENTAL DATA AND CALCULATIONS - Continued

Time $t-t_o$ (hrs)	$\frac{t-t_o}{t_s}$ (dimensionless)	Weight (grams)	Weight gain per unit area above W_o (grams/cm^2)	$\frac{V_f}{V_{ao}}$ (dimensionless)	Average saturation S (dimensionless)
			CORE NO. 13		
0.0	0.00000	63.88	0.0000	0.000	0.899
2.8	0.00545	64.08	0.0398	0.117	0.911
22.3	0.0411	64.40	0.103	0.304	0.930
47.3	0.0937	64.53	0.128	0.378	0.937
72.0	0.143	64.67	0.156	0.460	0.946
95.3	0.189	64.76	0.174	0.513	0.951
114.3	0.227	64.80	0.182	0.537	0.953
138.8	0.275	64.85	0.192	0.566	0.956
173.5	0.344	64.94	0.210	0.619	0.962
191.8	0.380	64.98	0.218	0.643	0.964
222.8	0.442	65.03	0.228	0.673	0.967
237.0	0.470	65.04	0.230	0.678	0.968
260.0	0.516	65.05	0.232	0.684	0.968
288.3	0.572	65.17	0.256	0.755	0.975
335.3	0.665	65.20	0.262	0.773	0.977
360.0	0.714	65.23	0.268	0.791	0.979
383.3	0.760	65.30	0.282	0.832	0.983
407.3	0.808	65.34	0.290	0.855	0.985
456.3	0.905	65.52	0.325	0.959	0.996
482.3	0.956	65.56	0.333	0.982	0.998
504.3	1.000	65.59	0.339	1.000	1.000
			CORE NO. 14		
0.0	0.000	164.05	0.000	0.000	0.871
40.0	0.0132	165.38	0.259	0.188	0.895
90.0	0.0298	165.68	0.318	0.231	0.901
206.0	0.0682	166.25	0.426	0.310	0.911
256.0	0.0847	166.52	0.481	0.350	0.916
326.0	0.108	166.75	0.526	0.382	0.920
422.0	0.140	167.13	0.600	0.436	0.927
676.0	0.224	167.82	0.734	0.533	0.940
744.0	0.246	168.10	0.788	0.573	0.945
998.0	0.330	168.64	0.883	0.642	0.955
1098.0	0.363	168.74	0.913	0.664	0.957
I343.0	0.444	169.31	1.024	0.744	0.967
1366.0	0.452	169.50	1.061	0.771	0.970
1596.0	0.528	169.63	1.086	0.789	0.973
1716.0	0.568	169.90	1.138	0.827	0.978
1836.0	0.608	170.00	1.158	0.842	0.980
1991.0	0.659	170.20	1.197	0.870	0.983
2182.0	0.722	170.48	1.251	0.909	0.988
2400.0	0.794	170.73	1.300	0.945	0.993
2571.0	0.851	170.83	1.320	0.959	0.995
2686.0	0.889	171.00	1.353	0.983	0.998
2980.0	0.986	171.03	1.358	0.987	0.998
3022.0	1.000	171.12	1.376	1.000	1.000
			CORE NO. 15		
0.0	0.0000	41.23	0.00000	0.000	0.927
16.0	0.0639	41.61	0.0733	0.294	0.949
24.1	0.0964	41.72	0.0945	0.384	0.955
55.1	0.220	42.01	0.149	0.608	0.972
77.5	0.310	42.17	0.180	0.735	0.981
102.7	0.411	42.28	0.202	0.824	0.987
125.9	0.503	42.34	0.213	0.869	0.991
147.9	0.591	42.40	0.226	0.922	0.994
199.3	0.797	42.47	0.239	0.976	0.998
250.1	1.000	42.50	0.245	1.000	1.000
			CORE NO. 16		
0.0	0.0000	41.22	0.0000	0.000	0.927
4.3	0.0102	41.41	0.0366	0.151	0.938

TABLE A-1. EXPERIMENTAL DATA AND CALCULATIONS - Continued

Time $t-t_o$ (hrs)	$\frac{t-t_o}{t_s}$ (dimensionless)	Weight (grams)	Weight gain per unit area above W_o (grams/cm^2)	$\frac{V_f}{V_{ao}}$ (dimensionless)	Average saturation S (dimensionless)
			CORE NO. 16 - Continued		
27.3	0.0642	41.63	0.0790	0.322	0.950
48.6	0.114	41.70	0.0925	0.380	0.954
97.6	0.229	41.85	0.122	0.498	0.963
123.8	0.291	41.95	0.141	0.576	0.969
145.6	0.342	42.01	0.152	0.620	0.972
169.6	0.398	42.07	0.164	0.669	0.976
194.1	0.456	42.13	0.176	0.718	0.979
222.6	0.523	42.25	0.199	0.812	0.986
241.6	0.568	42.30	0.208	0.849	0.989
267.1	0.628	42.30	0.208	0.849	0.989
289.6	0.680	42.34	0.216	0.882	0.991
337.6	0.793	42.41	0.230	0.939	0.995
380.6	0.894	42.45	0.237	0.967	0.998
401.6	0.944	42.47	0.241	0.984	0.999
425.6	1.000	42.49	0.245	1.000	1.000
			CORE NO. 17		
0.0	0.00000	41.21	0.0000	0.000	0.927
3.0	0.00703	41.36	0.0289	0.119	0.929
5.8	0.0135	41.42	0.0411	0.168	0.933
20.0	0.0468	41.59	0.0741	0.302	0.942
45.0	0.105	41.68	0.0906	0.370	0.948
65.0	0.152	41.79	0.112	0.457	0.954
70.5	0.165	41.80	0.114	0.465	0.955
90.0	0.211	41.83	0.120	0.490	0.957
100.0	0.234	41.95	0.143	0.584	0.964
116.0	0.272	41.95	0.143	0.584	0.964
137.0	0.321	41.97	0.147	0.600	0.965
162.0	0.379	42.03	0.158	0.645	0.974
188.0	0.440	42.10	0.172	0.702	0.978
210.0	0.492	42.15	0.181	0.739	0.981
234.0	0.548	42.20	0.191	0.780	0.982
258.0	0.604	42.22	0.195	0.796	0.983
307.0	0.719	42.33	0.216	0.882	0.991
331.0	0.775	42.37	0.224	0.914	0.994
354.0	0.829	42.39	0.228	0.931	0.995
379.0	0.888	42.40	0.230	0.939	0.995
404.0	0.946	42.46	0.239	0.976	0.999
426.9	1.000	42.49	0.245	1.000	1.000
			CORE NO. 18		
0.0	0.000	41.23	0.000	0.000	0.927
76.0	0.183	41.86	0.121	0.494	0.963
96.0	0.231	41.90	0.129	0.522	0.965
124.0	0.299	42.08	0.142	0.580	0.970
147.0	0.354	42.10	0.149	0.608	0.971
172.0	0.414	42.19	0.166	0.678	0.976
196.0	0.472	42.21	0.170	0.694	0.978
220.0	0.530	42.30	0.207	0.844	0.988
289.0	0.696	42.38	0.222	0.906	0.993
316.0	0.761	42.41	0.228	0.931	0.995
340.0	0.819	42.41	0.228	0.931	0.995
364.0	0.877	42.43	0.232	0.947	0.996
387.0	0.933	42.46	0.237	0.967	0.998
415.0	1.000	42.50	0.245	1.000	1.000
			CORE NO. 19		
0.0	0.00000	33.68	0.000	0.000	0.952
4.3	0.00851	33.78	0.0208	0.148	0.959
9.5	0.0188	33.82	0.0291	0.206	0.962
21.5	0.0426	33.89	0.0436	0.309	0.967
29.0	0.0574	33.91	0.0478	0.339	0.969

TABLE A-1. EXPERIMENTAL DATA AND CALCULATIONS - Continued

Time $t-t_o$ (hrs)	$\frac{t-t_o}{t_s}$ (dimensionless)	Weight (grams)	Weight gain per unit area above W_o (grams/cm^2)	$\frac{V_f}{V_{ao}}$ (dimensionless)	Average saturation S (dimensionless)
			CORE NO. 19 - Continued		
44.0	0.0871	33.91	0.0478	0.339	0.969
53.0	0.105	33.95	0.0561	0.398	0.972
68.5	0.136	33.99	0.0644	0.457	0.974
77.0	0.152	34.00	0.0665	0.472	0.975
91.0	0.180	34.00	0.0665	0.472	0.975
101.0	0.200	34.01	0.0686	0.487	0.975
125.0	0.248	34.07	0.0810	0.574	0.980
176.0	0.348	34.11	0.0894	0.634	0.982
188.0	0.372	34.11	0.0894	0.634	0.982
211.0	0.418	34.12	0.0914	0.648	0.983
235.0	0.465	34.16	0.0997	0.707	0.986
259.0	0.513	34.19	0.106	0.752	0.988
284.0	0.562	34.21	0.110	0.780	0.989
310.0	0.614	34.20	0.108	0.766	0.987
335.0	0.663	34.22	0.112	0.794	0.990
357.0	0.707	34.26	0.121	0.858	0.993
381.0	0.754	34.27	0.123	0.872	0.994
451.0	0.893	34.33	0.135	0.957	0.998
480.5	0.951	34.33	0.135	0.957	0.998
505.0	1.000	34.36	0.141	1.000	1.000
			CORE NO. 20		
0.0	0.00000	30.97	0.000	0.000	0.936
4.3	0.00813	31.05	0.0182	0.0943	0.942
9.5	0.0180	31.11	0.0318	0.165	0.947
21.5	0.0406	31.18	0.0454	0.235	0.952
29.0	0.0548	31.20	0.0522	0.270	0.954
44.0	0.0832	31.21	0.0545	0.282	0.954
53.0	0.100	31.23	0.0590	0.306	0.956
68.5	0.129	31.25	0.0636	0.330	0.957
77.0	0.146	31.30	0.0749	0.388	0.961
91.0	0.172	31.32	0.0795	0.412	0.963
101.0	0.191	31.32	0.0795	0.412	0.963
125.0	0.236	31.39	0.0953	0.494	0.968
176.0	0.333	31.44	0.107	0.554	0.972
188.0	0.355	31.49	0.118	0.611	0.975
211.0	0.399	31.50	0.120	0.622	0.976
235.0	0.444	31.51	0.123	0.637	0.977
259.0	0.491	31.59	0.141	0.731	0.983
284.0	0.537	31.59	0.141	0.731	0.983
310.0	0.586	31.59	0.141	0.731	0.983
335.0	0.633	31.65	0.154	0.798	0.987
381.0	0.720	31.70	0.166	0.860	0.991
451.0	0.853	31.74	0.175	0.907	0.994
480.5	0.908	31.78	0.184	0.953	0.997
505.0	0.955	31.79	0.186	0.964	0.998
529.0	1.000	31.82	0.193	1.000	1.000
			CORE NO. 21		
0.0	0.00000	35.27	0.000	0.000	0.951
4.3	0.00813	35.37	0.0199	0.136	0.958
9.5	0.0180	35.42	0.0299	0.205	0.961
21.5	0.0406	35.50	0.0459	0.314	0.967
29.0	0.0548	35.52	0.0499	0.342	0.969
44.0	0.0832	35.50	0.0459	0.314	0.968
53.0	0.100	35.54	0.0539	0.369	0.969
68.5	0.129	35.55	0.0559	0.383	0.970
77.0	0.146	35.61	0.0678	0.464	0.974
91.0	0.172	35.60	0.0658	0.451	0.973
101.0	0.191	35.61	0.0678	0.464	0.974
125.0	0.236	35.68	0.0818	0.560	0.979
176.0	0.333	35.70	0.0858	0.588	0.980
188.0	0.355	35.70	0.0858	0.588	0.980

TABLE A-1. EXPERIMENTAL DATA AND CALCULATIONS - Continued

Time $t-t_o$ (hrs)	$\frac{t-t_o}{t_s}$ (dimensionless)	Weight (grams)	Weight gain per unit area above W_o (grams/cm^2)	$\frac{V_f}{V_{ao}}$ (dimensionless)	Average saturation S (dimensionless)
		CORE NO. 21 - Continued			
211.0	0.399	35.73	0.0918	0.629	0.982
235.0	0.444	35.76	0.0977	0.669	0.984
259.0	0.491	35.79	0.104	0.712	0.986
284.0	0.537	35.81	0.108	0.740	0.987
310.0	0.586	35.81	0.108	0.740	0.987
335.0	0.633	35.88	0.122	0.836	0.992
381.0	0.720	35.89	0.124	0.949	0.993
451.0	0.853	35.95	0.136	0.932	0.997
480.5	0.908	35.98	0.142	0.973	0.999
505.0	0.955	35.97	0.140	0.959	0.998
529.0	1.000	36.00	0.146	1.000	1.000
		CORE NO. 22			
0.0	0.00000	31.60	0.0000	0.000	0.933
4.3	0.00813	31.69	0.0199	0.100	0.939
9.5	0.0180	31.73	0.0287	0.144	0.942
21.5	0.0406	31.80	0.0442	0.222	0.948
29.0	0.0548	31.82	0.0486	0.244	0.949
44.0	0.0832	31.82	0.0486	0.244	0.949
53.0	0.100	31.88	0.0618	0.311	0.954
68.5	0.129	31.90	0.0662	0.333	0.955
77.0	0.146	31.93	0.0729	0.366	0.957
91.0	0.172	31.94	0.0751	0.377	0.958
101.0	0.191	31.97	0.0817	0.411	0.960
125.0	0.236	32.02	0.0927	0.466	0.964
176.0	0.333	32.09	0.108	0.538	0.969
188.0	0.355	32.10	0.110	0.553	0.970
211.0	0.399	32.13	0.117	0.588	0.972
235.0	0.444	32.18	0.128	0.643	0.976
259.0	0.491	32.21	0.135	0.678	0.978
284.0	0.537	32.27	0.148	0.744	0.983
310.0	0.586	32.27	0.148	0.744	0.983
335.0	0.633	32.31	0.157	0.789	0.986
381.0	0.720	32.35	0.166	0.834	0.989
451.0	0.853	32.42	0.181	0.910	0.994
480.5	0.908	32.47	0.192	0.965	0.998
505.0	0.955	32.48	0.194	0.975	0.998
529.0	1.000	32.50	0.199	1.000	1.000

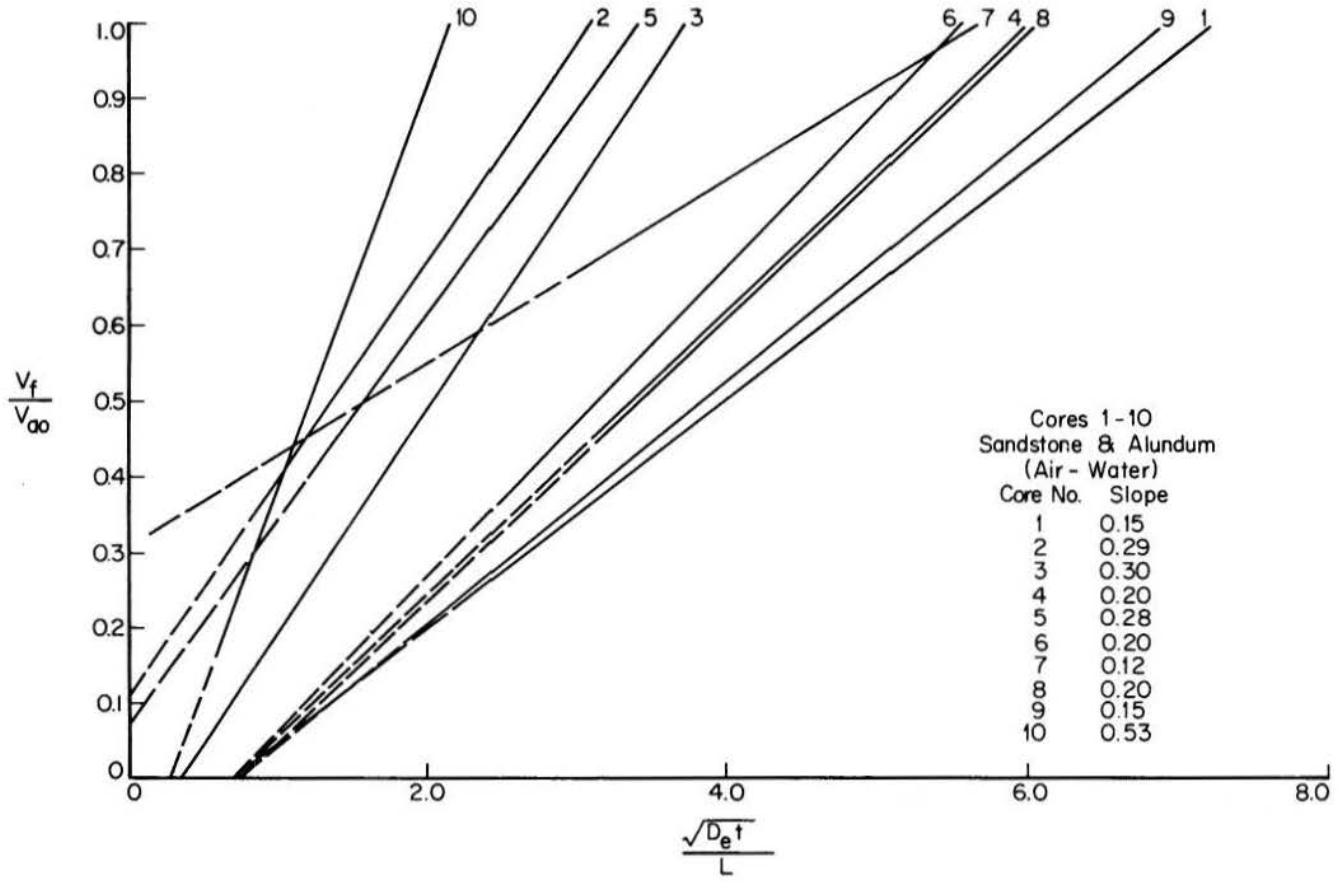

Figure B-1. V_f/V_{ao} as a function of $(D_e t/L^2)^{\frac{1}{2}}$

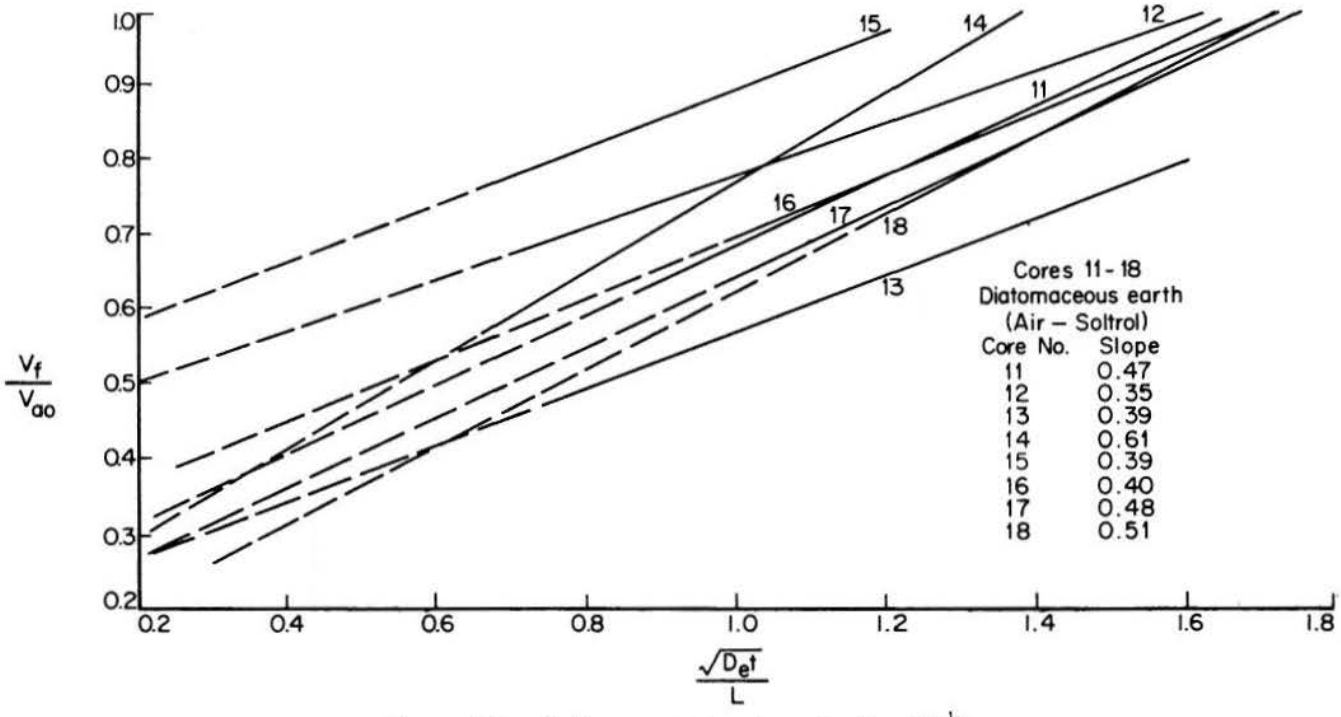

Figure B-2. V_f/V_{ao} as a function of $(D_e t/L^2)^{\frac{1}{2}}$

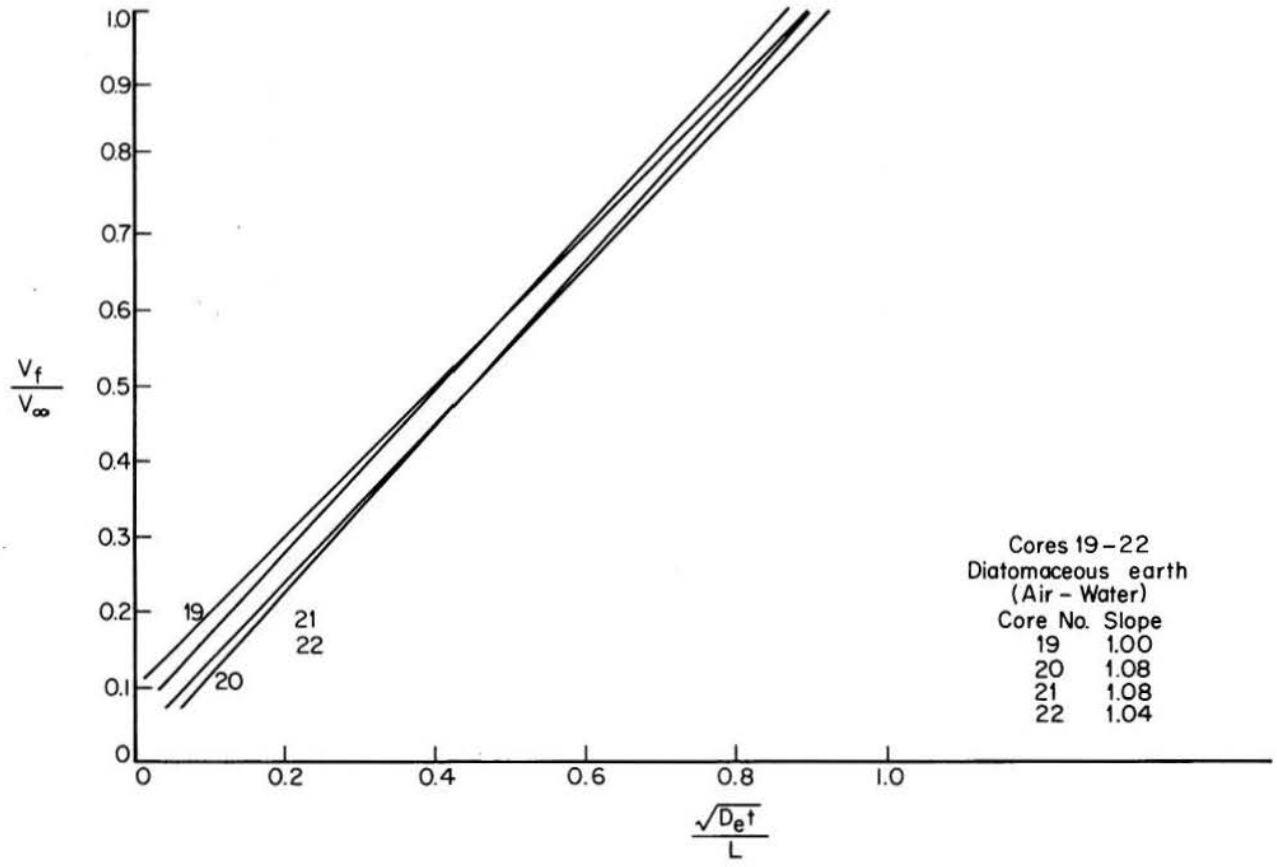

Figure B-3. V_f/V_{ao} as a function of $(D_e t/L^2)^{\frac{1}{2}}$

TABLE B-1. ACTUAL AND THEORETICAL SLOPES USING BLOCMSBURG'S METHOD

Core No.	Measured Slope	Calculated Slope $\frac{2C_o}{(1-S_o)\phi}\frac{\rho_\ell}{\rho_a}$	$\frac{\text{Measured Slope}}{\text{Calculated Slope}}$	Calculated $\alpha \times 10^6$ from Eq. 11*
1	0.15	0.13	1.15	6.24
2	0.29	0.80	0.36	5.61
3	0.30	0.36	0.83	8.32
4	0.20	0.19	1.05	5.19
5	0.28	0.26	1.08	14.78
6	0.20	0.23	0.87	5.90
7	0.12	0.20	0.60	6.41
8	0.20	1.17	0.17	0.63
9	0.15	0.26	0.58	2.62
10	0.53	0.31	1.71	19.94
11	0.47	3.80	0.12	4.28
12	0.35	3.98	0.08	4.54
13	0.39	3.91	0.10	3.21
14	0.61	3.00	0.23	2.38
15	0.39	5.40	0.07	4.84
16	0.40	5.40	0.07	2.72
17	0.48	5.40	0.09	2.72
18	0.51	5.40	0.09	2.80
19	1.00	0.58	1.72	-17.28
20	1.08	0.43	2.51	-12.62
21	1.08	0.56	1.93	-17.06
22	1.04	0.40	2.60	-13.27

*Corrected for tortuosity

APPENDIX C

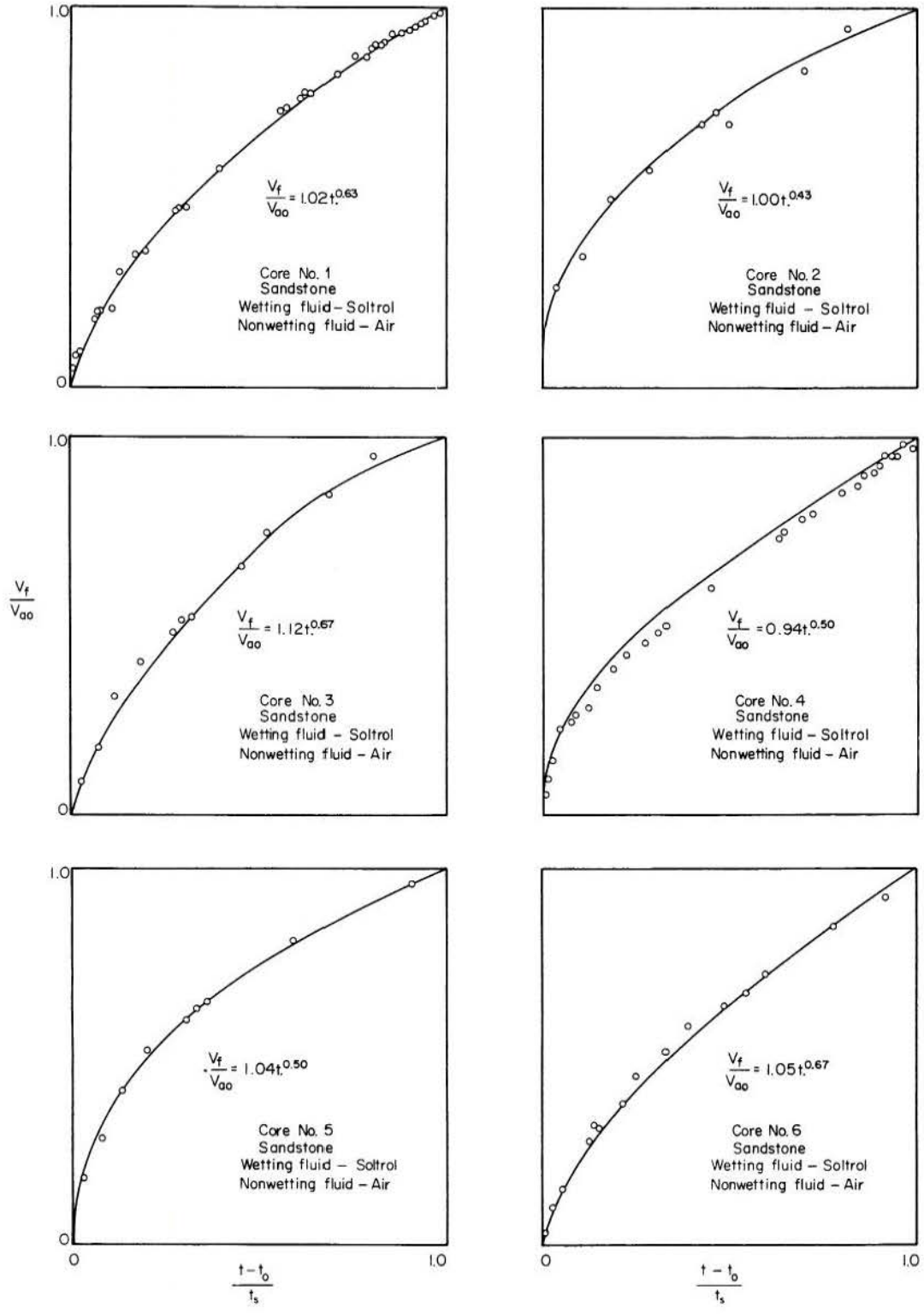

Figure C-1. V_f/V_{ao} as a function of dimensionless time

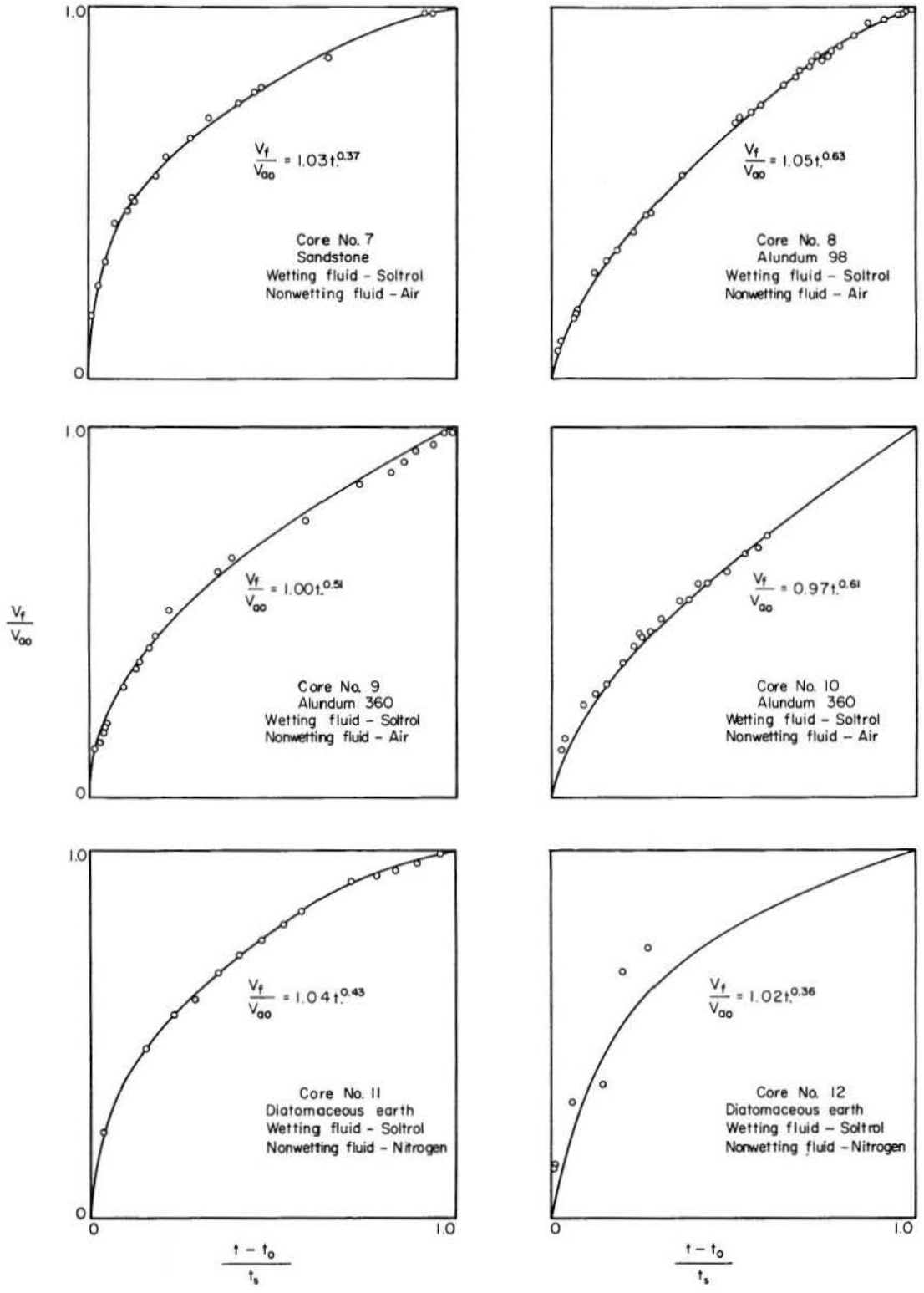

Figure C-1. V_f/V_{ao} as a function of dimensionless time - Continued

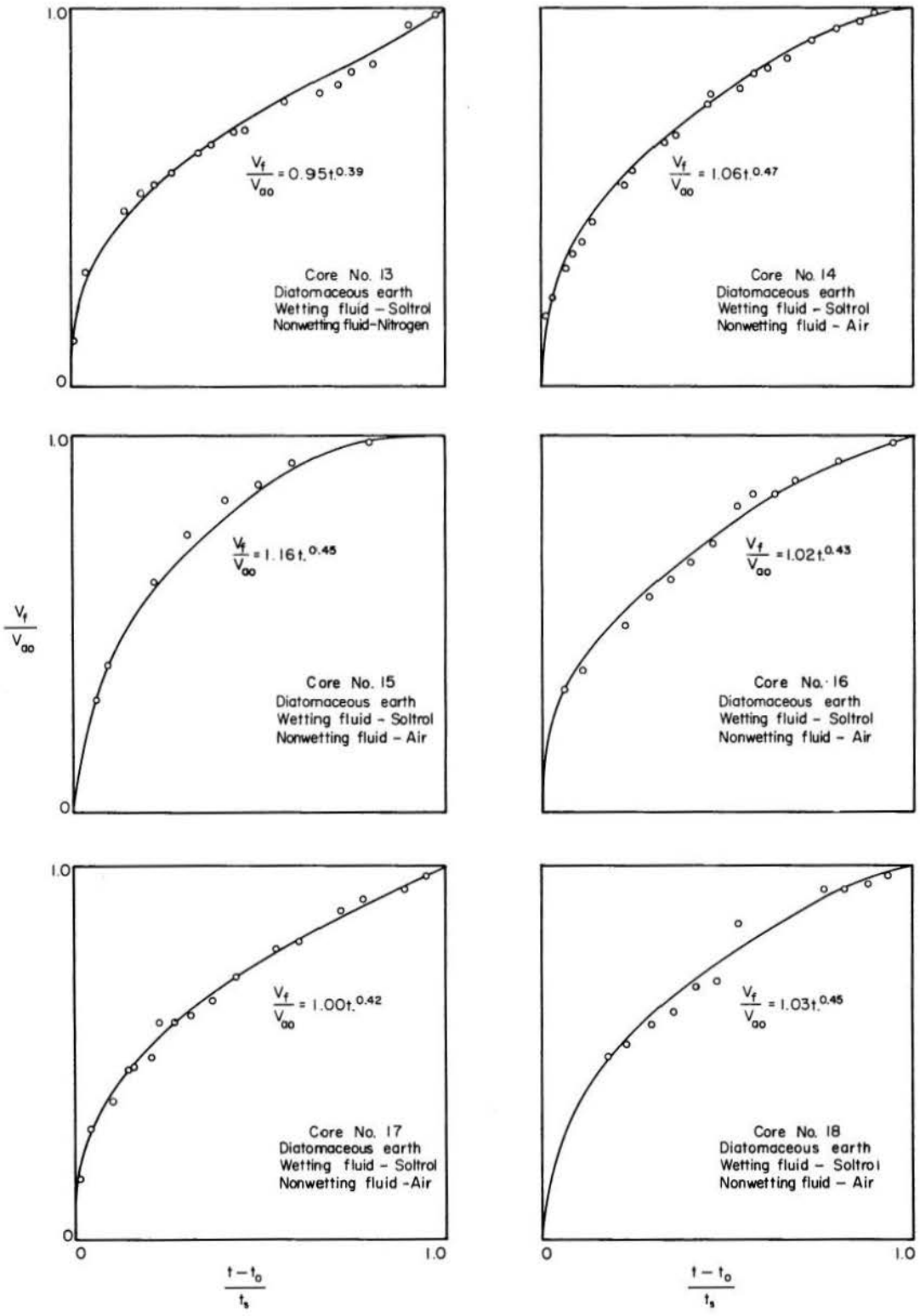

Figure C-1. V_f/V_{ao} as a function of dimensionless time - Continued

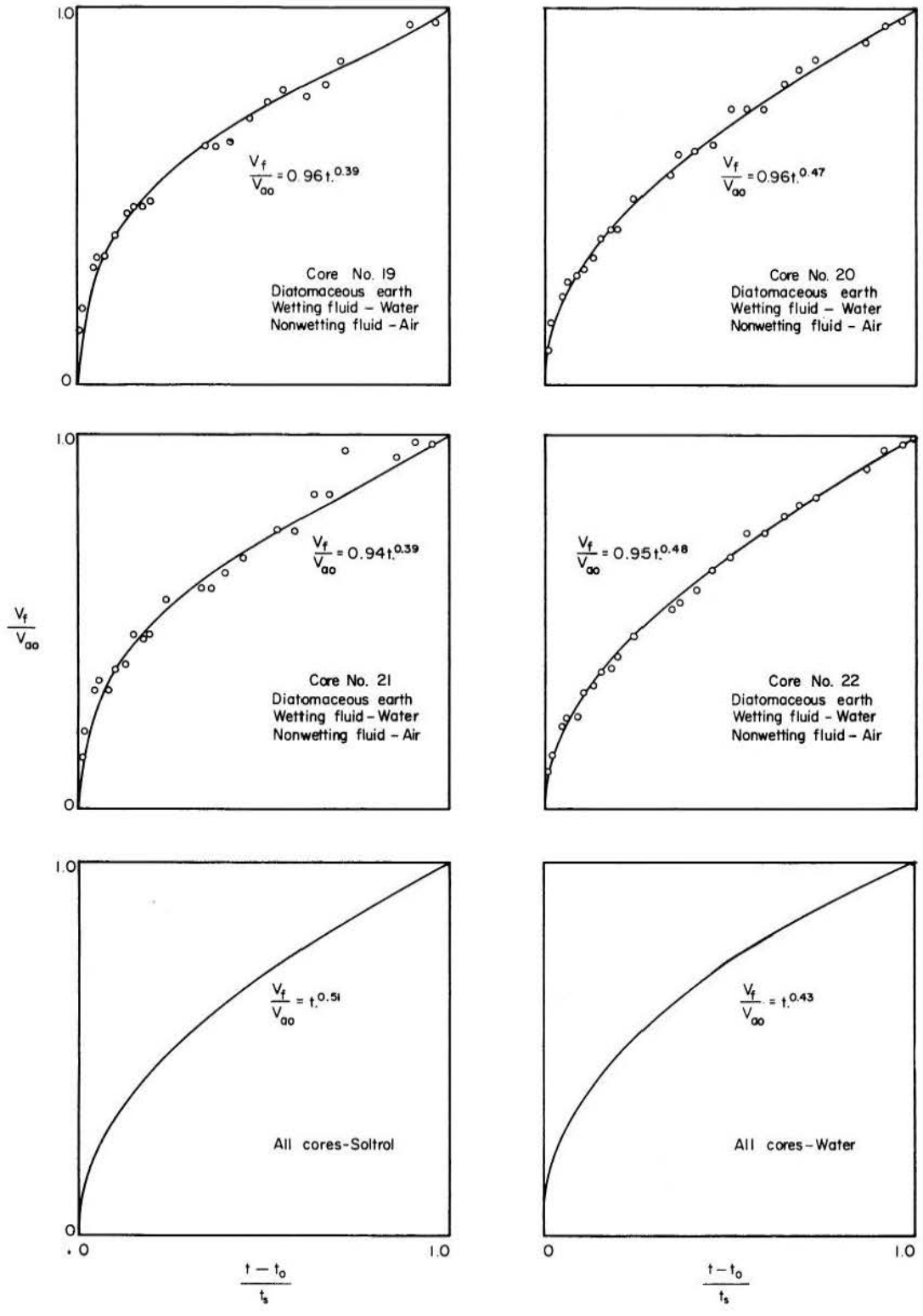

Figure C-1. V_f/V_{ao} as a function of dimensionless time - Continued

Key Words: Diffusion, Unidirectional diffusion, Entrapped gas, Porous media, Interfacial energy.

Abstract: Equations are developed and tested that describe the process whereby a gas which is in isolated pockets surrounded by a liquid, diffuses from a porous medium and is replaced by liquid. The equation developed by Bloomsburg for the case of unidirectional diffusion and a similar equation developed by introducing one simplifying assumption beyond those made by Bloomsburg were tested. Experimental results show that neither of these developments adequately describe the process.

A graphical method of estimating rates of diffusion, developed from observing the trends of experimental data, is given. It is based upon extrapolation of experimental data obtained using cores from the material of interest. Besides giving the time at which full liquid saturation would occur, this method allows the liquid distribution to be estimated at any time from normalized curves which relate air content to dimensionless length and dimensionless time.

Reference: Adam, Kenneth M., and Corey, Arthur T., Colorado State University, Hydrology Paper No. 27 (April 1968), "Diffusion of Entrapped Gas from Porous Media."

Key Words: Diffusion, Unidirectional diffusion, Entrapped gas, Porous media, Interfacial energy.

Abstract: Equations are developed and tested that describe the process whereby a gas which is in isolated pockets surrounded by a liquid, diffuses from a porous medium and is replaced by liquid. The equation developed by Bloomsburg for the case of unidirectional diffusion and a similar equation developed by introducing one simplifying assumption beyond those made by Bloomsburg were tested. Experimental results show that neither of these developments adequately describe the process.

A graphical method of estimating rates of diffusion, developed from observing the trends of experimental data, is given. It is based upon extrapolation of experimental data obtained using cores from the material of interest. Besides giving the time at which full liquid saturation would occur, this method allows the liquid distribution to be estimated at any time from normalized curves which relate air content to dimensionless length and dimensionless time.

Reference: Adam, Kenneth M., and Corey, Arthur T., Colorado State University, Hydrology Paper No. 27 (April 1968), "Diffusion of Entrapped Gas from Porous Media."

Key Words: Diffusion, Unidirectional diffusion, Entrapped gas, Porous media, Interfacial energy.

Abstract: Equations are developed and tested that describe the process whereby a gas which is in isolated pockets surrounded by a liquid, diffuses from a porous medium and is replaced by liquid. The equation developed by Bloomsburg for the case of unidirectional diffusion and a similar equation developed by introducing one simplifying assumption beyond those made by Bloomsburg were tested. Experimental results show that neither of these developments adequately describe the process.

A graphical method of estimating rates of diffusion, developed from observing the trends of experimental data, is given. It is based upon extrapolation of experimental data obtained using cores from the material of interest. Besides giving the time at which full liquid saturation would occur, this method allows the liquid distribution to be estimated at any time from normalized curves which relate air content to dimensionless length and dimensionless time.

Reference: Adam, Kenneth M., and Corey, Arthur T., Colorado State University, Hydrology Paper No. 27 (April 1968), "Diffusion of Entrapped Gas from Porous Media."

Key Words: Diffusion, Unidirectional diffusion, Entrapped gas, Porous media, Interfacial energy.

Abstract: Equations are developed and tested that describe the process whereby a gas which is in isolated pockets surrounded by a liquid, diffuses from a porous medium and is replaced by liquid. The equation developed by Bloomsburg for the case of unidirectional diffusion and a similar equation developed by introducing one simplifying assumption beyond those made by Bloomsburg were tested. Experimental results show that neither of these developments adequately describe the process.

A graphical method of estimating rates of diffusion, developed from observing the trends of experimental data, is given. It is based upon extrapolation of experimental data obtained using cores from the material of interest. Besides giving the time at which full liquid saturation would occur, this method allows the liquid distribution to be estimated at any time from normalized curves which relate air content to dimensionless length and dimensionless time.

Reference: Adam, Kenneth M., and Corey, Arthur T., Colorado State University, Hydrology Paper No. 27 (April 1968), "Diffusion of Entrapped Gas from Porous Media."

PREVIOUSLY PUBLISHED PAPERS

Colorado State University Hydrology Papers

No. 18 "Stochastic Model of Daily River Flow Sequences," by Rafael G. Quimpo, February 1967.

No. 19 "Engineering Judgment and Small Area Flood Peaks," by Lourens A. V. Hiemstra and Brian M. Reich, April 1967.

No. 20 "Accuracy of Discharge Determinations," by W. T. Dickinson, June 1967.

No. 21 "Water Quality of Mountain Watersheds," by Samuel H. Kunkle and James R. Meiman, June 1967.

No. 22 "Prediction of Water Yield in High Mountain Watersheds Based on Physiography," by Robert W. Julian, Vujica Yevjevich, and Hubert J. Morel-Seytoux, August 1967.

No. 23 "An Objective Approach to Definitions and Investigations of Continental Hydrologic Droughts," by Vujica Yevjevich, August 1967.

No. 24 "Application of Cross-Spectral Analysis to Hydrologic Time Series," by Ignacio Rodriguez-Iturbe, September 1967.

No. 25 "An Experimental Rainfall-Runoff Facility," by W. T. Dickinson, M. E. Holland and G. L. Smith, September 1967.

No. 26 "The Investigation of Relationship Between Hydrologic Time Series and Sunspot Numbers," by Ignacio Rodriguez-Iturbe and Vujica Yevjevich, April 1968.

Colorado State University Fluid Mechanics Papers

No. 4 "Experiment on Wind Generated Waves on the Water Surface of a Laboratory Channel," by E. J. Plate and C. S. Yang, February 1966.

No. 5 "Investigations of the Thermally Stratified Boundary Layer," by E. J. Plate and C. W. Lin, February 1966.

No. 6 "Atmospheric Diffusion in the Earth's Boundary Layer--Diffusion in the Vertical Direction and Effects of the Thermal Stratification," by Shozo Ito, February 1966.

Colorado State University Hydraulics Papers

No. 1 "Design of Conveyance Channels in Alluvial Materials," by D. B. Simons, March 1966.

No. 2 "Diffusion of Slot Jets with Finite Orifice Length-Width Ratios," by V. Yevjevich, March 1966.

No. 3 "Dispersion of Mass in Open-Channel Flow," by William W. Sayre, February 1968.